


# Normal approximations for the multivariate inverse Gaussian distribution and asymmetric kernel smoothing on $d$ -dimensional half-spaces

Léo R. Belzile<sup>1</sup> , Alain Desgagné<sup>2</sup>   
Christian Genest<sup>3</sup>  and Frédéric Ouimet<sup>3</sup> 

<sup>1</sup>*Département de sciences de la décision, HEC Montréal*  
e-mail: [leo.belzile@hec.ca](mailto:leo.belzile@hec.ca)

<sup>2</sup>*Département de mathématiques, Université du Québec à Montréal*  
e-mail: [desgagne.alain@uqam.ca](mailto:desgagne.alain@uqam.ca)

<sup>3</sup>*Department of Mathematics and Statistics, McGill University*  
e-mail: [christian.genest@mcgill.ca](mailto:christian.genest@mcgill.ca); [frederic.ouimet2@mcgill.ca](mailto:frederic.ouimet2@mcgill.ca)

**Abstract:** This paper introduces a novel density estimator supported on  $d$ -dimensional half-spaces. It stands out as the first asymmetric kernel smoother for half-spaces in the literature. Using the multivariate inverse Gaussian (MIG) density from Minami (2003) as the kernel and incorporating locally adaptive parameters, the estimator achieves desirable boundary properties. To analyze its mean integrated squared error (MISE) and asymptotic normality, a local limit theorem and probability metric bounds are established between the MIG and the corresponding multivariate Gaussian distribution with the same mean vector and covariance matrix, which may also be of independent interest. Additionally, a new algorithm for generating MIG random vectors is developed, proving to be faster and more accurate than Minami's algorithm based on a Brownian hitting location representation. This algorithm is then used to discuss and compare optimal MISE and likelihood cross-validation bandwidths for the estimator in a simulation study under various target distributions. As an illustration, the MIG asymmetric kernel is used to smooth the posterior distribution of a generalized Pareto model fitted to large electromagnetic storms.

**MSC2020 subject classifications:** Primary 62G07; secondary 62E15, 62E20, 62G05, 62H10, 62H12.

**Keywords and phrases:** Asymmetric kernel, asymptotic theory, density estimation, Gaussian approximation, half-space, local limit theorem, multivariate inverse Gaussian distribution, multivariate normal distribution, normal approximation, simulation algorithm, smoothing.

---

**Contents**

1	Introduction . . . . .	3
2	Objectives, outline, and notation . . . . .	4
	2.1 Objectives . . . . .	4
	2.2 Outline . . . . .	4
	2.3 Notation . . . . .	5
3	Normal approximations . . . . .	5
	3.1 The univariate case . . . . .	5
	3.2 The multivariate case . . . . .	8
4	Exact simulation algorithm . . . . .	11
5	The MIG asymmetric kernel smoother . . . . .	14
	5.1 Asymptotic results . . . . .	15
	5.2 Simulation study . . . . .	19
	5.2.1 Results . . . . .	21
	5.3 Real-data application . . . . .	24
A	Proofs of the normal approximations . . . . .	26
	A.1 Proofs in the univariate case . . . . .	26
	A.1.1 Proof of Theorem 3.1 . . . . .	26
	A.1.2 Proof of Theorem 3.2 . . . . .	27
	A.2 Proofs in the multivariate case . . . . .	28
	A.2.1 Proof of Theorem 3.3 . . . . .	28
	A.2.2 Proof of Theorem 3.4 . . . . .	29
B	Distribution function evaluation for MIG vectors . . . . .	30
	B.1 General strategy . . . . .	30
	B.2 Integration bounds in dimension $d = 2$ . . . . .	32
	B.3 Integration bounds in dimension $d \geq 3$ . . . . .	34
C	Proofs of the asymptotics for the MIG asymmetric kernel smoother . . . . .	35
	C.1 Proof of Proposition 5.1 . . . . .	35
	C.2 Proof of Proposition 5.2 . . . . .	35
	C.3 Proof of Theorem 5.5 . . . . .	37
D	Technical lemmas . . . . .	38
	D.1 Uniform bound on the MIG density . . . . .	38
	D.2 Maximum likelihood estimator (MLE) . . . . .	39
	D.3 Hessian of the MIG density . . . . .	41
E	Reproducibility . . . . .	41
F	List of abbreviations . . . . .	41
	Funding . . . . .	42
	References . . . . .	42

---

## 1. Introduction

The inverse Gaussian (IG) distribution is a versatile stochastic model that is often used to model data with positive support and skewness. It was first introduced by [Wald \(1944\)](#) as a limiting distribution in the context of sequential probability ratio tests. Since then, it has found a large number of applications in a variety of fields, including actuarial science, demography, engineering, medicine, and environmental sciences, among others; see [Seshadri \(1999\)](#) for a review.

Various multivariate extensions of the IG distribution can be found in the literature. An early example is due to [Al-Hussaini and Abd-El-Hakim \(1981\)](#), who constructed a bivariate family with IG margins by exploiting an idea of [Parzen \(1960\)](#); however, the range of values for Pearson's correlation in their model depends on the marginal parameters. Alternatively, [Barndorff-Nielsen and Blæsild \(1983\)](#) defined reproductive exponential families and proposed bivariate IG models through a conditional approach which is convenient for analysis of variance, but their distributions do not have IG margins.

Bivariate IG distributions have also been derived from stochastic processes. In [Iyengar \(1985\)](#), a possible extension arises naturally from the joint law of certain hitting times for the components of a driftless Brownian motion. An earlier proposal had been made by [Wasan \(1968\)](#), who investigated a specific continuous-time stochastic process with an IG distribution at each point in time. [Kocherlakota \(1986\)](#), who corrected and generalized this work, derived the basic properties of this model. For a review of bivariate IG distributions, refer to Section 11.21 of [Balakrishnan and Lai \(2009\)](#).

In arbitrary dimension  $d \geq 2$ , flexible models with (possibly generalized) IG margins are more difficult to build. [Barndorff-Nielsen, Blæsild and Seshadri \(1992\)](#) proposed one such method, which involves Poisson mixtures to generate the dependence structure. [Joe, Seshadri and Arnold \(2012\)](#) mention the possibility of constructing such models by combining IG margins with a copula ([Genest and Nešlehová, 2012](#)), but their own extension, which is closed under marginalization, is based instead on a stochastic representation of the IG distribution using a transform of a  $t_2$ -skewed normal distribution.

In practice, however, the multivariate inverse Gaussian (MIG) distribution that has been most often used is due to [Minami \(2003\)](#); see, e.g., [Tang et al. \(2007\)](#), [Tang et al. \(2009\)](#), [Masuadi \(2013\)](#), [Zhang, Yan and Liu \(2019\)](#), [Sahoo and Dash \(2021\)](#), and [Kumar, Yadav and Kumar \(2021\)](#). Minami's construction, which is based on a reduced inverse relationship with multivariate Gaussian distributions, allows for easy derivations of its mean vector, covariance matrix, and higher-order cumulants. It is also reproductive, infinitely divisible, closed under linear transformations, and occurs as a limiting case of the multivariate Lagrange distribution ([Minami, 2007](#)). Moreover, this distribution is easy to simulate from, as it is characterized as the location of a correlated Brownian motion hitting a certain hyperplane for the first time. All this makes Minami's MIG distribution a valuable tool for a wide range of statistical applications. It is the version studied in this paper.

## 2. Objectives, outline, and notation

### 2.1. Objectives

The first objective of the present work is to prove a local limit theorem and to derive probability metric bounds between the MIG distribution introduced by [Minami \(2003\)](#) and the multivariate normal distribution with the same mean vector and covariance matrix. For ease of reading, and also because the corresponding univariate results were not found in the literature, the local limit theorem and probability metric bounds are stated and proved in one dimension under a slightly different (but more common) parametrization.

The second objective is to develop a new algorithm for generating MIG random vectors that is faster and more accurate than the one proposed by [Minami \(2003\)](#), who exploited the aforementioned Brownian hitting location representation. This work builds on the characterization of the MIG from [Minami \(2003\)](#) as a transformation of a location and scale mixture of Gaussian vectors, with inverse Gaussian driving noise. The same stochastic representation also enables the provision of an estimator of the distribution function via importance sampling in two dimensions ( $d = 2$ ).

The third objective is to introduce a novel density estimator supported on  $d$ -dimensional half-spaces. It stands out as the first asymmetric kernel smoother for half-spaces in the literature. The local limit theorem is employed to derive some of its asymptotic properties. The new algorithm facilitates drawing samples for the Monte Carlo estimation of optimal bandwidth matrices. In particular, optimal MISE and likelihood cross-validation bandwidths for the estimator are discussed and compared in a simulation study under various target distributions. The practical utility of the MIG asymmetric kernel smoother is shown in a bivariate application involving smoothing the posterior distribution of a generalized Pareto model fitted to large electromagnetic storms.

### 2.2. Outline

The rest of this paper is organized as follows. In [Section 3.1](#), the IG distribution ( $d = 1$ ) is defined and the corresponding local limit theorem and probability metric bounds are stated. In [Section 3.2](#), the MIG distribution ( $d \geq 1$ ) of [Minami \(2003\)](#) is defined and the corresponding local limit theorem and probability metric bounds are stated. The proofs are deferred to [Appendix A](#).

The new algorithm for generating MIG random vectors is given in [Section 4](#). In [Appendix B](#), the stochastic representation at the core of this algorithm is leveraged to evaluate the distribution function of MIG random vectors.

Next, the MIG asymmetric kernel smoother with positive definite bandwidth matrix  $\mathbf{H}$  is introduced in [Section 5](#). Its asymptotic properties are stated in [Section 5.1](#) and proved in [Appendix C](#). Some technical lemmas used in the proofs are relegated to [Appendix D](#). A simulation study is conducted in [Section 5.2](#), and a real-data application is investigated in [Section 5.3](#). Informations concerning

the R code for the simulations are provided in Appendix E. For easy reference, a list of the abbreviations employed in the paper appears in Appendix F.

### 2.3. Notation

In Section 5 and the related proofs, the matrix notations  $\|\cdot\|_2$ ,  $|\cdot|$  and  $\text{tr}(\cdot)$  denote the spectral norm, determinant and trace, respectively. For a given dimension  $d \in \mathbb{N}$ , the quantities  $\mathbf{0}_d$ ,  $\mathbf{1}_d$ , and  $\mathbf{I}_d$ , denote a  $d$ -vector of zeros, a  $d$ -vector of 1s, and the identity matrix of width  $d$ , respectively. The notation  $\mathcal{S}_{++}^d$  stands for the space of (real) symmetric positive definite matrices of size  $d \times d$ .

Throughout the paper, the notation  $u = \mathcal{O}(v)$  means that  $\limsup |u/v| \leq C < \infty$  as  $\lambda/\mu \rightarrow \infty$  or  $\mu/\omega \rightarrow \infty$  or  $n \rightarrow \infty$  or  $\|\mathbf{H}\|_2 \rightarrow 0$ , depending on the context, where the positive constant  $C \in (0, \infty)$  may depend on the target density  $f$  or the dimension  $d$  but no other variable unless explicitly written as a subscript. Similarly, the notation  $u = o(v)$  means that  $\lim |u/v| = 0$  as  $\lambda/\mu \rightarrow \infty$  or  $\mu/\omega \rightarrow \infty$  or  $n \rightarrow \infty$  or  $\|\mathbf{H}\|_2 \rightarrow 0$ . Subscripts indicate which parameters the convergence rate can depend on. Convergence in distribution is denoted using the squiggly arrow  $\rightsquigarrow$ .

## 3. Normal approximations

### 3.1. The univariate case

Consider the following parametrization of the inverse Gaussian distribution, as defined, e.g., in Chapter 15 of Johnson, Kotz and Balakrishnan (1994). For any positive reals  $\mu, \lambda \in (0, \infty)$ , a random variable  $X$  is said to be  $\text{IG}(\mu, \lambda)$ -distributed, and one writes  $X \sim \text{IG}(\mu, \lambda)$ , if its density function is given, for all  $x \in (0, \infty)$ , by

$$k_{\mu, \lambda}(x) = \sqrt{\frac{\lambda}{2\pi x^3}} \exp\left\{-\frac{\lambda(x - \mu)^2}{2\mu^2 x}\right\}. \quad (3.1)$$

The expectation and variance are well known to be

$$\mathbb{E}(X) = \mu, \quad \text{Var}(X) = \frac{\mu^3}{\lambda}; \quad (3.2)$$

see, e.g., Section 15.4 of Johnson, Kotz and Balakrishnan (1994).

In order to relate the univariate density (3.1) more easily to its multivariate generalization in Section 3.2, one can use the alternative parametrization given, for all  $x \in (0, \infty)$ , by

$$k_{\mu, \mu^2/\omega}(x) = \frac{\mu}{\sqrt{2\pi\omega x^3}} \exp\left\{-\frac{(x - \mu)^2}{2\omega x}\right\}, \quad (3.3)$$

where  $\mu \in (0, \infty)$  as before and  $\omega = \mu^2/\lambda \in (0, \infty)$ . Under this new parametrization, the expectation and variance become

$$\mathbb{E}(X) = \mu, \quad \text{Var}(X) = \mu\omega.$$

The last two equations can be compared with their multivariate analog in (3.11) and (3.12), where the vector parameter  $\beta$  is set to 1 for simplicity.

It is well known that if  $X \sim \text{IG}(\mu, \lambda)$ , then, as  $\lambda/\mu \rightarrow \infty$ , or equivalently as  $\mu/\omega \rightarrow \infty$ , one has

$$\delta_X \equiv \frac{X - \mu}{\sqrt{\mu^3/\lambda}} \rightsquigarrow \mathcal{N}(0, 1); \quad (3.4)$$

see, e.g., (Seshadri, 1999, p. 5).

The purpose of this section is to study, as  $\lambda/\mu \rightarrow \infty$ , the local distance at a given point  $x$  between the inverse Gaussian density  $k_{\mu,\lambda}(x)$  and the Gaussian density  $\phi_{\mu,\mu^3/\lambda}(x)$  which has the same mean and variance. The latter is defined, for all  $x \in \mathbb{R}$ , by

$$\phi_{\mu,\mu^3/\lambda}(x) = \sqrt{\frac{\lambda}{2\pi\mu^3}} \exp\left\{-\frac{\lambda(x-\mu)^2}{2\mu^3}\right\}. \quad (3.5)$$

As long as  $x$  is located in the *bulk* of the inverse Gaussian distribution (i.e., not too far from the mean  $\mu$ ), the terms in the series expansion of the log-ratio  $\ln\{k_{\mu,\lambda}(x)/\phi_{\mu,\mu^3/\lambda}(x)\}$  will be shown explicitly in Theorem 3.1, along with the rate of convergence of any truncation.

For any  $\mu, \lambda \in (0, \infty)$  and  $\tau \in (0, \sqrt{\lambda/\mu}]$ , the bulk of radius  $\tau$  for the inverse Gaussian distribution, and its closure, are defined, respectively, by

$$\begin{aligned} B_{\mu,\lambda}(\tau) &= \{x \in (0, \infty) : |\delta_x| < \tau\}, \\ \overline{B_{\mu,\lambda}}(\tau) &= \{x \in (0, \infty) : |\delta_x| \leq \tau\}. \end{aligned}$$

Note that, by selecting  $\tau$  large enough, the probability that  $X \sim \text{IG}(\mu, \lambda)$  lands into the bulk region  $B_{\mu,\lambda}(\tau)$  has probability arbitrarily close to 1 as  $\lambda/\mu \rightarrow \infty$ .

**Theorem 3.1** (Local limit theorem). *For any positive reals  $\mu, \lambda \in (0, \infty)$  and  $x \in B_{\mu,\lambda}(\sqrt{\lambda/\mu})$ , one has*

$$LR(x) \equiv \ln\left\{\frac{k_{\mu,\lambda}(x)}{\phi_{\mu,\mu^3/\lambda}(x)}\right\} = \sum_{k=1}^{\infty} (-1)^k \left(\frac{3}{2k} - \frac{\delta_x^2}{2}\right) \left(\delta_x \sqrt{\frac{\mu}{\lambda}}\right)^k. \quad (3.6)$$

Furthermore, given any integer  $n \in \mathbb{N}$  and any real  $\tau \in (0, \sqrt{\lambda/\mu})$ , one has, uniformly for all  $x \in \overline{B_{\mu,\lambda}}(\tau)$  and as  $\lambda/\mu \rightarrow \infty$ ,

$$LR(x) - \sum_{k=1}^{n-1} (-1)^k \left(\frac{3}{2k} - \frac{\delta_x^2}{2}\right) \left(\delta_x \sqrt{\frac{\mu}{\lambda}}\right)^k = \mathcal{O}_{\tau}\left\{\left(\frac{\mu}{\lambda}\right)^{n/2}\right\}. \quad (3.7)$$

In particular, if  $n = 1$ , one has, as  $\lambda/\mu \rightarrow \infty$ ,

$$LR(x) = \mathcal{O}_{\tau}\left(\sqrt{\frac{\mu}{\lambda}}\right). \quad (3.8)$$

Govindarajulu (1965) was the first to derive explicit local approximations akin to those in Theorem 3.1 for the Poisson, binomial and negative binomial distributions. These approximations were based on Fourier analysis results from Esseen (1945). The Fourier analysis approach is now ubiquitous in statistics; see, e.g., Kolassa (1994) for a general reference.

An elementary approach using Taylor expansions and Stirling’s formula was later introduced by Cressie (1978) to obtain similar local approximations for the binomial distribution as well as refined continuity corrections. Non-asymptotic version of Cressie’s results were derived by Ouimet (2022) to improve Tusnády’s inequality in the bulk, a critical component in demonstrating the Komlós–Major–Tusnády approximation that controls the deviations between the empirical process and an appropriate sequence of Brownian bridges on the same probability space. The approach of Cressie was also adapted by Ouimet (2023) to the negative binomial setting in order to study the asymptotics of the median and settle a problem left open by Coeurjolly and Trépanier (2020). The proof of Theorem 3.1 relies on a similar elementary approach; see Appendix A.1.

Below, graphical evidence is provided for the validity of the log-ratio expansion in Theorem 3.1. Three levels of approximation are compared for the case  $\lambda = \mu^2$  (or equivalently,  $\omega = 1$ ). Define

$$\begin{aligned} E_1 &= \sup_{x \in \overline{B_{\mu, \lambda}(1)}} |LR(x)|, \\ E_2 &= \sup_{x \in \overline{B_{\mu, \lambda}(1)}} \left| LR(x) + \left( \frac{3}{2} - \frac{\delta_x^2}{2} \right) \left( \delta_x \sqrt{\frac{\mu}{\lambda}} \right) \right|, \\ E_3 &= \sup_{x \in \overline{B_{\mu, \lambda}(1)}} \left| LR(x) + \left( \frac{3}{2} - \frac{\delta_x^2}{2} \right) \left( \delta_x \sqrt{\frac{\mu}{\lambda}} \right) - \left( \frac{3}{4} - \frac{\delta_x^2}{2} \right) \left( \delta_x \sqrt{\frac{\mu}{\lambda}} \right)^2 \right|. \end{aligned}$$

Recall that  $x \in \overline{B_{\mu, \lambda}(1)}$  implies  $|\delta_x| \leq 1$ , so one expects from (3.7) that the maximal errors  $E_n$  above will have, for every integer  $n \in \{1, 2, 3\}$ , the asymptotic behavior

$$\frac{1}{E_n} = \mathcal{O} \left\{ \left( \frac{\mu}{\lambda} \right)^{-n/2} \right\} = \mathcal{O}(\mu^{n/2}) \Leftrightarrow \liminf_{\mu \rightarrow \infty} \frac{-\ln(E_n)}{\ln(\mu)} \geq \frac{n}{2}. \quad (3.9)$$

The two equivalent properties in (3.9) are illustrated on the left-hand side and right-hand side of Figure 1, respectively. For a link to the R code used to generate this figure, refer to Appendix E.

By applying the local approximations of Theorem 3.1 in the bulk and by showing that the contributions outside the bulk are negligible using concentration inequalities, probability metric bounds between the measures induced by the densities  $k_{\mu, \lambda}$  and  $\phi_{\mu, \mu^3/\lambda}$  are established. The following is a global result.

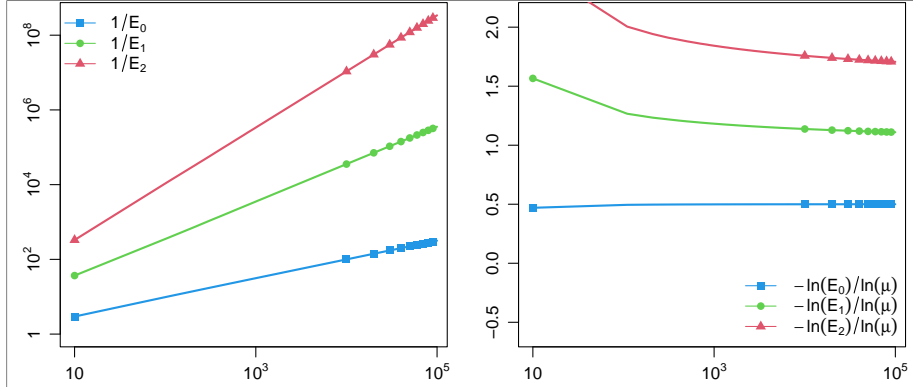


FIG 1. The plot on the left-hand side displays  $1/E_n$  as a function of  $\mu$ , utilizing a logarithmic scale for both the horizontal and vertical axes. It illustrates the improvement achieved by incorporating correction terms from Theorem 3.1 to the base approximation. On the right-hand side, the plot displays  $-\ln(E_n)/\ln(\mu)$  as a function of  $\mu$ , with the horizontal axis logarithmically scaled. The plot confirms the asymptotic orders of the liminf in (3.9) and provides compelling numerical evidence for the validity of Theorem 3.1.

**Theorem 3.2** (Probability metric bounds). *Let  $P_{\mu,\lambda}$  be the measure on  $\mathbb{R}$  induced by the IG density  $k_{\mu,\lambda}$  in (3.1). Let  $Q_{\mu,\lambda}$  be the measure on  $\mathbb{R}$  induced by the Gaussian density  $\phi_{\mu,\mu^3/\lambda}$  in (3.5). Then, for any positive reals  $\mu, \lambda \in (0, \infty)$ , one has*

$$H(P_{\mu,\lambda}, Q_{\mu,\lambda}) \leq C \sqrt{\frac{\mu}{\lambda}}, \quad (3.10)$$

where  $C \in (0, \infty)$  is a universal constant and  $H(\cdot, \cdot)$  denotes the Hellinger distance. The bound (3.10) is also valid if one replaces the Hellinger distance by any of the following probability metrics: Discrepancy metric, Kolmogorov (or Uniform) metric, Lévy metric, Prokhorov metric, Total variation.

### 3.2. The multivariate case

The following multivariate extension of the inverse Gaussian distribution (3.1), referred to as the MIG distribution, was proposed by Minami (2003) and further studied in Minami (2007). For any integer  $d \in \mathbb{N}$  (the dimension), let  $\beta, \xi \in \mathbb{R}^d$  be vectors such that  $\beta^\top \xi \in (0, \infty)$ , and let  $\Omega \in \mathcal{S}_{++}^d$  be a symmetric positive definite matrix of size  $d \times d$ . A random vector  $\mathbf{X}$  is said to be  $\text{MIG}(\beta, \xi, \Omega)$ -distributed, and one writes  $\mathbf{X} \sim \text{MIG}(\beta, \xi, \Omega)$ , if its density function is given, for all  $\mathbf{x} \in \mathcal{H}_d(\beta) = \{\mathbf{x} \in \mathbb{R}^d : \beta^\top \mathbf{x} \in (0, \infty)\}$ , by

$$k_{\beta,\xi,\Omega}(\mathbf{x}) = (2\pi)^{-d/2} \beta^\top \xi |\Omega|^{-1/2} (\beta^\top \mathbf{x})^{-(d/2+1)} \times \exp \left\{ -\frac{1}{2\beta^\top \mathbf{x}} (\mathbf{x} - \xi)^\top \Omega^{-1} (\mathbf{x} - \xi) \right\}. \quad (3.11)$$



The support  $\mathcal{H}_d(\boldsymbol{\beta})$  is called a half-space; it contains the vectors  $\boldsymbol{x}$  which have the ‘same general direction’ as the fixed parameter  $\boldsymbol{\beta}$  in the sense that their scalar product is positive. The expectation and covariance matrix of the MIG distribution are

$$\mathbf{E}(\mathbf{X}) = \boldsymbol{\xi}, \quad \text{Var}(\mathbf{X}) = \boldsymbol{\beta}^\top \boldsymbol{\xi} \boldsymbol{\Omega}, \quad (3.12)$$

as stated in Property 1 of [Minami \(2003\)](#).

In order to study the limiting behavior of the density function (3.11), the notation is extended by setting  $\boldsymbol{\xi} = \mu \boldsymbol{\xi}_0$  and  $\boldsymbol{\Omega} = \omega \boldsymbol{\Omega}_0$ , where the factors  $\mu, \omega \in (0, \infty)$  are positive reals, the vector  $\boldsymbol{\xi}_0 \in \mathbb{R}^d$  satisfies  $\boldsymbol{\beta}^\top \boldsymbol{\xi}_0 \in (0, \infty)$ , and  $\boldsymbol{\Omega}_0 \in \mathcal{S}_{++}^d$  is a symmetric positive definite matrix of size  $d \times d$ . Set  $d = \boldsymbol{\beta} = \boldsymbol{\xi}_0 = \boldsymbol{\Omega}_0 = \mathbf{1}$  to obtain the univariate density function in (3.3).

It is known that if  $\mathbf{X} \sim \text{MIG}(\boldsymbol{\beta}, \mu \boldsymbol{\xi}_0, \omega \boldsymbol{\Omega}_0)$ , then, as  $\mu/\omega \rightarrow \infty$ , one has

$$\boldsymbol{\delta}_{\mathbf{X}} \equiv (\mu\omega \boldsymbol{\beta}^\top \boldsymbol{\xi}_0)^{-1/2} \mathbf{L}_0^{-1} (\mathbf{X} - \mu \boldsymbol{\xi}_0) \rightsquigarrow \mathcal{N}_d(\mathbf{0}_d, \mathbf{I}_d), \quad (3.13)$$

where  $\mathbf{L}_0$  is the lower triangular matrix in the Cholesky decomposition  $\boldsymbol{\Omega}_0 = \mathbf{L}_0 \mathbf{L}_0^\top$ . This is a straightforward consequence of the expression for the MIG cumulant generating function in Theorem 1 of [Minami \(2003\)](#) combined with Lévy’s continuity theorem for Laplace transforms; see, e.g., ([Feller, 1971](#), p. 431).

As in the univariate case, the goal is to study, as  $\mu/\omega \rightarrow \infty$ , the local distance at a given point  $\boldsymbol{x}$  between the MIG density  $k_{\boldsymbol{\beta}, \mu \boldsymbol{\xi}_0, \omega \boldsymbol{\Omega}_0}(\boldsymbol{x})$  and the corresponding multivariate normal density with the same mean vector and covariance matrix, the latter being defined, for all  $\boldsymbol{x} \in \mathbb{R}^d$ , by

$$\begin{aligned} \phi_{\mu \boldsymbol{\xi}_0, \mu \omega \boldsymbol{\beta}^\top \boldsymbol{\xi}_0 \boldsymbol{\Omega}_0}(\boldsymbol{x}) &= (2\pi)^{-d/2} (\mu\omega \boldsymbol{\beta}^\top \boldsymbol{\xi}_0)^{-d/2} |\boldsymbol{\Omega}_0|^{-1/2} \\ &\times \exp \left\{ -\frac{1}{2\mu\omega \boldsymbol{\beta}^\top \boldsymbol{\xi}_0} (\boldsymbol{x} - \mu \boldsymbol{\xi}_0)^\top \boldsymbol{\Omega}_0^{-1} (\boldsymbol{x} - \mu \boldsymbol{\xi}_0) \right\}. \end{aligned} \quad (3.14)$$

In particular, as long as  $\boldsymbol{x}$  is located in the *bulk* of the MIG distribution (i.e., not too far from the mean  $\mu \boldsymbol{\xi}_0$ ), the terms in the series expansion of the log-ratio  $\ln\{k_{\boldsymbol{\beta}, \mu \boldsymbol{\xi}_0, \omega \boldsymbol{\Omega}_0}(\boldsymbol{x})/\phi_{\mu \boldsymbol{\xi}_0, \mu \omega \boldsymbol{\beta}^\top \boldsymbol{\xi}_0 \boldsymbol{\Omega}_0}(\boldsymbol{x})\}$  will be shown explicitly in Theorem 3.3, along with the rate of convergence of any truncation. This result rests indirectly on the fact that the MIG distribution is infinitely divisible, as stated in Property 4 of [Minami \(2003\)](#).

For any positive reals  $\mu, \omega \in (0, \infty)$  and  $\tau \in (0, \sqrt{\mu/\omega}]$ , the bulk of radius  $\tau$  for the MIG distribution, and its closure, are defined, respectively, by

$$\begin{aligned} B_{\mu, \omega, \boldsymbol{\beta}, \boldsymbol{\xi}_0, \boldsymbol{\Omega}_0}(\tau) &= \left\{ \boldsymbol{x} \in \mathcal{H}_d(\boldsymbol{\beta}) : \frac{|\boldsymbol{\beta}^\top \boldsymbol{\Omega}_0^{1/2} \boldsymbol{\delta}_{\boldsymbol{x}}|}{\sqrt{\boldsymbol{\beta}^\top \boldsymbol{\xi}_0}} < \tau \right\}, \\ \overline{B_{\mu, \omega, \boldsymbol{\beta}, \boldsymbol{\xi}_0, \boldsymbol{\Omega}_0}}(\tau) &= \left\{ \boldsymbol{x} \in \mathcal{H}_d(\boldsymbol{\beta}) : \frac{|\boldsymbol{\beta}^\top \boldsymbol{\Omega}_0^{1/2} \boldsymbol{\delta}_{\boldsymbol{x}}|}{\sqrt{\boldsymbol{\beta}^\top \boldsymbol{\xi}_0}} \leq \tau \right\}. \end{aligned}$$

Note that, by selecting a large enough  $\tau$ , the probability that  $\mathbf{X} \sim \text{MIG}(\boldsymbol{\beta}, \boldsymbol{\xi}, \boldsymbol{\Omega})$  lands into the bulk region  $B_{\mu, \omega, \boldsymbol{\beta}, \boldsymbol{\xi}_0, \boldsymbol{\Omega}_0}(\tau)$  has probability arbitrarily close to 1 as  $\mu/\omega \rightarrow \infty$ .

**Theorem 3.3** (Local limit theorem). *Let the real vectors  $\beta \in \mathbb{R}^d$ ,  $\xi_0 \in \mathcal{H}_d(\beta)$ , and the symmetric positive definite matrix  $\Omega_0 \in \mathcal{S}_{++}^d$ , be given. For any positive reals  $\mu, \omega \in (0, \infty)$  and any real vector  $\mathbf{x} \in B_{\mu, \omega, \beta, \xi_0, \Omega_0}(\sqrt{\mu/\omega})$ , one has*

$$\begin{aligned} LR(\mathbf{x}) &\equiv \ln \left\{ \frac{k_{\beta, \mu \xi_0, \omega \Omega_0}(\mathbf{x})}{\phi_{\mu \xi_0, \mu \omega \beta^\top \xi_0 \Omega_0}(\mathbf{x})} \right\} \\ &= \sum_{k=1}^{\infty} (-1)^k \left( \frac{d+2}{2k} - \frac{\delta_{\mathbf{x}}^\top \delta_{\mathbf{x}}}{2} \right) \left( \frac{\beta^\top \Omega_0^{1/2} \delta_{\mathbf{x}}}{\sqrt{\beta^\top \xi_0}} \sqrt{\frac{\omega}{\mu}} \right)^k. \end{aligned} \quad (3.15)$$

Furthermore, given any integer  $n \in \mathbb{N}$  and any real  $\tau \in (0, \sqrt{\mu/\omega})$ , one has, uniformly for  $\mathbf{x} \in \overline{B_{\mu, \omega, \beta, \xi_0, \Omega_0}}(\tau)$  and as  $\mu/\omega \rightarrow \infty$ ,

$$\begin{aligned} LR(\mathbf{x}) &- \sum_{k=1}^{n-1} (-1)^k \left( \frac{d+2}{2k} - \frac{\delta_{\mathbf{x}}^\top \delta_{\mathbf{x}}}{2} \right) \left( \frac{\beta^\top \Omega_0^{1/2} \delta_{\mathbf{x}}}{\sqrt{\beta^\top \xi_0}} \sqrt{\frac{\omega}{\mu}} \right)^k \\ &= \mathcal{O}_{\tau, \beta, \xi_0, \Omega_0} \left\{ \left( \frac{\omega}{\mu} \right)^{n/2} \right\}. \end{aligned} \quad (3.16)$$

In particular, if  $n = 1$ , one has, as  $\mu/\omega \rightarrow \infty$ ,

$$LR(\mathbf{x}) = \mathcal{O}_{\tau, \beta, \xi_0, \Omega_0} \left( \sqrt{\frac{\omega}{\mu}} \right). \quad (3.17)$$

Graphical evidence is provided below for the validity of the log-ratio expansion in Theorem 3.3 when  $d = 2$ ,  $\beta = (1/2, 1/2)^\top$  and  $\xi_0 = (1, 1)^\top$ , so that  $\beta^\top \xi_0 = 1$  in particular. The case  $(\mu \rightarrow \infty, \omega = 1)$  is considered. Three levels of approximation are compared for various choices of  $\Omega_0$ . Define

$$\begin{aligned} E_1 &= \sup_{\mathbf{x} \in \overline{B_{\mu, \omega, \beta, \xi_0, \Omega_0}}(1)} |LR(\mathbf{x})|, \\ E_2 &= \sup_{\mathbf{x} \in \overline{B_{\mu, \omega, \beta, \xi_0, \Omega_0}}(1)} \left| LR(\mathbf{x}) + \left( \frac{d+2}{2} - \frac{\delta_{\mathbf{x}}^\top \delta_{\mathbf{x}}}{2} \right) \left( \frac{\beta^\top \Omega_0^{1/2} \delta_{\mathbf{x}}}{\sqrt{\beta^\top \xi_0}} \sqrt{\frac{\omega}{\mu}} \right) \right|, \\ E_3 &= \sup_{\mathbf{x} \in \overline{B_{\mu, \omega, \beta, \xi_0, \Omega_0}}(1)} \left| LR(\mathbf{x}) + \left( \frac{d+2}{2} - \frac{\delta_{\mathbf{x}}^\top \delta_{\mathbf{x}}}{2} \right) \left( \frac{\beta^\top \Omega_0^{1/2} \delta_{\mathbf{x}}}{\sqrt{\beta^\top \xi_0}} \sqrt{\frac{\omega}{\mu}} \right) \right. \\ &\quad \left. - \left( \frac{d+2}{4} - \frac{\delta_{\mathbf{x}}^\top \delta_{\mathbf{x}}}{2} \right) \left( \frac{\beta^\top \Omega_0^{1/2} \delta_{\mathbf{x}}}{\sqrt{\beta^\top \xi_0}} \sqrt{\frac{\omega}{\mu}} \right)^2 \right|. \end{aligned}$$

Recall that  $\mathbf{x} \in \overline{B_{\mu, \omega, \beta, \xi_0, \Omega_0}}(1)$  implies  $|\beta^\top \Omega_0^{1/2} \delta_{\mathbf{x}}| / (\beta^\top \xi_0)^{1/2} \leq 1$ , so one expects from (3.16) that the maximal errors  $E_n$  above will have, for every integer  $n \in \{1, 2, 3\}$ , the asymptotic behavior

$$\frac{1}{E_n} = \mathcal{O}_{\beta, \xi_0, \Omega_0} \left\{ \left( \frac{\omega}{\mu} \right)^{-n/2} \right\} = \mathcal{O}_{\beta, \xi_0, \Omega_0} (\mu^{n/2})$$

$$\Leftrightarrow \liminf_{\mu \rightarrow \infty} \frac{-\ln(E_n)}{\ln(\mu)} \geq \frac{n}{2}. \quad (3.18)$$

The two equivalent properties in (3.18) are illustrated in Figure 2 and Figure 3, respectively, for various choices of  $\Omega_0$ .

By applying the local approximations of Theorem 3.3 in the bulk and by showing that the contributions coming from outside the bulk are negligible using concentration inequalities, probability metric bounds between the measures induced by the densities  $k_{\beta, \mu \xi_0, \omega \Omega_0}$  and  $\phi_{\mu \xi_0, \mu \omega \beta^\top \xi_0 \Omega_0}$  are established. The following is a global result.

**Theorem 3.4** (Probability metric bounds). *Let  $P_{\mu, \omega, \beta, \xi_0, \Omega_0}$  be the measure on  $\mathbb{R}^d$  induced by the MIG density  $k_{\beta, \mu \xi_0, \omega \Omega_0}$  in (3.11). Let  $Q_{\mu, \omega, \beta, \xi_0, \Omega_0}$  be the measure on  $\mathbb{R}^d$  induced by multivariate Gaussian density  $\phi_{\mu \xi_0, \mu \omega \beta^\top \xi_0 \Omega_0}$  in (3.14). Then, for any positive reals  $\mu, \omega \in (0, \infty)$ , one has*

$$H(P_{\mu, \omega, \beta, \xi_0, \Omega_0}, Q_{\mu, \omega, \beta, \xi_0, \Omega_0}) \leq C \sqrt{\frac{\omega}{\mu}}, \quad (3.19)$$

where  $C = C(d, \beta, \xi_0, \Omega_0) \in (0, \infty)$  is a positive constant that may depend on  $d, \beta, \xi_0$  and  $\Omega_0$ , and  $H(\cdot, \cdot)$  denotes the Hellinger distance. The bound (3.19) is also valid if one replaces the Hellinger distance by any of the following probability metrics: Discrepancy metric, Kolmogorov (or Uniform) metric, Lévy metric, Prokhorov metric, Total variation.

#### 4. Exact simulation algorithm

This section describes a new algorithm for generating MIG random vectors which is faster than the one proposed by Minami (2003), who exploited the Brownian hitting location representation mentioned in Section 1. A separation-of-variable algorithm is also proposed to efficiently evaluate the distribution function of the MIG using sequential importance sampling. Both methods rely on Theorem 1 (3) of Minami (2003).

**Proposition 4.1** (Sampling from the MIG distribution). *Let  $\beta \in \mathbb{R}^d$  be the vector defining the half-space  $\mathcal{H}_d(\beta)$  and consider a  $(d-1) \times d$  matrix  $\mathbf{Q}_2$ , such that  $\mathbf{Q}_2^\top \beta = \mathbf{0}_{d-1}$  and  $\mathbf{Q}_2 \mathbf{Q}_2^\top = \mathbf{I}_{d-1}$ . Theorem 1 (3) of Minami (2003) states that, if  $\mathbf{Q} = (\beta, \mathbf{Q}_2^\top)^\top$  and*

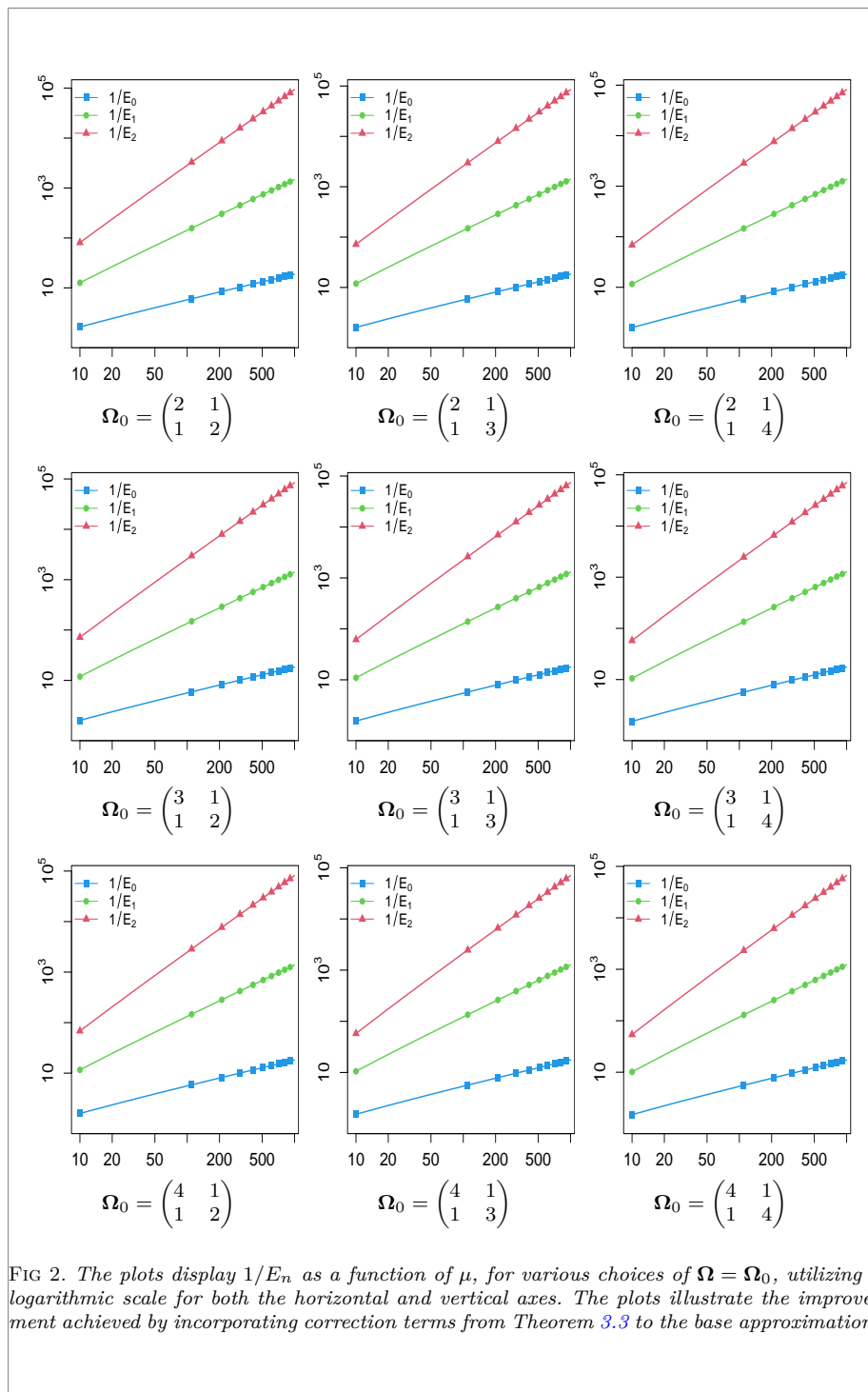
$$R \sim \text{IG}[\beta^\top \xi, (\beta^\top \xi)^2 / (\beta^\top \Omega \beta)],$$

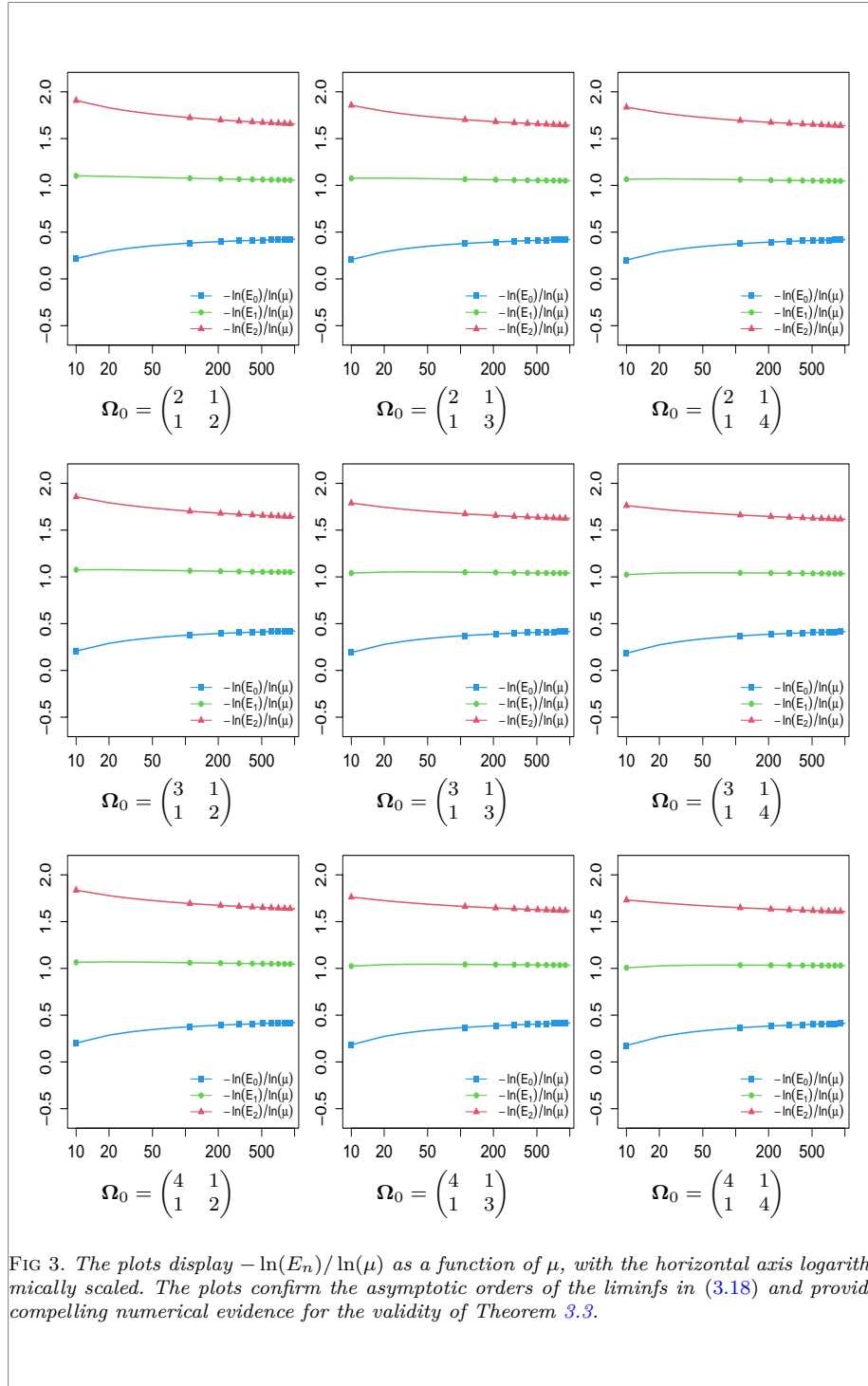
$$\mathbf{Z} \mid R = r \sim \mathcal{N}_{d-1}[\boldsymbol{\mu}(r), r \boldsymbol{\Sigma}], \quad (4.1)$$

where

$$\boldsymbol{\mu}(r) = \mathbf{Q}_2 \{ \xi + \Omega \beta (\beta^\top \Omega \beta)^{-1} (r - \beta^\top \xi) \}, \quad \boldsymbol{\Sigma} = (\mathbf{Q}_2 \Omega^{-1} \mathbf{Q}_2^\top)^{-1}, \quad (4.2)$$

then  $(R, \mathbf{Z}^\top)^\top$  is equal in distribution to  $\mathbf{Q} \mathbf{X}$ , where  $\mathbf{X} \sim \text{MIG}(\beta, \xi, \Omega)$ . As the mapping is invertible, it follows that  $\mathbf{Q}^{-1}(R, \mathbf{Z}^\top)^\top \sim \text{MIG}(\beta, \xi, \Omega)$ .





To construct  $\mathbf{Q}$ , the symmetric orthogonal projection matrix  $\mathbf{M}_\beta = \mathbf{I}_d - \beta\beta^\top / (\beta^\top\beta)$  of rank  $d - 1$  is considered. The  $(d - 1) \times d$  matrix  $\mathbf{Q}_2$  is built from the set of  $d - 1$  eigenvectors associated with the non-zero eigenvalues of  $\mathbf{M}_\beta$ . The inverse of  $\mathbf{Q}$  can then be computed via its singular value decomposition: given that  $\mathbf{Q}$  has  $d - 1$  singular values equal to 1 and one strictly positive, the linear mapping is invertible. An inverse Gaussian random variable  $R$  can then be sampled using the R package `statmod` (Giner and Smyth, 2016) and, conditional on the latter, a  $(d - 1)$ -Gaussian vector  $\mathbf{Z}$  as in (4.1) can be sampled. Then  $\mathbf{X} = \mathbf{Q}^{-1}(R, \mathbf{Z}^\top)^\top \sim \text{MIG}(\beta, \xi, \Omega)$  by Proposition 4.1.

**Remark 4.1.** The benefit of this approach, relative to the characterization as the hitting location of a correlated Brownian motion on a hyperplane (Minami, 2003, Theorem 2), is that the method is exact; the latter is only approximate because the time step for the Brownian motion needs to be discretized. Minami’s method is also several orders of magnitude slower than Proposition 4.1.

**Remark 4.2.** As simulation is cheap, the distribution function of a MIG distribution can be readily estimated via Monte Carlo by drawing vectors from the corresponding model. It is tempting to leverage the same stochastic representation to evaluate  $\Pr(\mathbf{X} \leq \mathbf{q})$ , where  $\mathbf{X} \sim \text{MIG}(\beta, \xi, \Omega)$ , using sequential importance sampling (e.g., Genz and Bretz, 2009) for the Gaussian component. Unfortunately, the linear transformation  $\mathbf{Q}_2$  of the region of integration,  $(-\infty_d, \mathbf{q}] \cap \mathcal{H}_d(\beta)$ , gives rise to a polytope and obtaining the transformed region of integration requires solving repeated linear programs, making the approach uncompetitive beyond the bivariate case, for which explicit expressions can be derived for the integration bounds. More details are provided in Appendix B.

## 5. The MIG asymmetric kernel smoother

Let  $\mathbf{X}_1, \dots, \mathbf{X}_n$  be a random sample from a common density function  $f$ , referred to as the target density, supported on the  $d$ -dimensional half-space

$$\mathcal{H}_d(\beta) = \{\mathbf{x} \in \mathbb{R}^d : \beta^\top \mathbf{x} \in (0, \infty)\}.$$

For a given symmetric positive definite bandwidth matrix  $\mathbf{H} \in \mathcal{S}_{++}^d$ , the MIG asymmetric kernel smoother for  $f$  is defined, for all  $\xi \in \mathcal{H}_d(\beta)$ , by

$$\hat{f}_{n, \mathbf{H}}(\xi) = \frac{1}{n} \sum_{i=1}^n k_{\beta, \xi, \mathbf{H}}(\mathbf{X}_i). \quad (5.1)$$

If the observations were supported on the translated half-space  $\mathbf{a} + \mathcal{H}_d(\beta)$  for some real vector  $\mathbf{a} \in \mathbb{R}^d$ , then one would replace each observation  $\mathbf{X}_i$  by the translated observation  $\mathbf{X}_i = \mathbf{X}_i - \mathbf{a}$  in (5.1).

The density estimator  $\hat{f}_{n, \mathbf{H}}$  is the first and only example in the literature of an asymmetric kernel smoother tailored for general half-spaces in dimension  $d \geq 2$ . For the one-dimensional analog on the half-line  $(0, \infty)$ , see, e.g., Scaillet (2004) and Bouezmarni and Scaillet (2005).

Asymmetric kernel estimators possess several desirable qualities. They offer distinct advantages by eliminating boundary bias asymptotically, as evidenced by Proposition 5.2 below, and by having no spill-over effect near the boundary because the shape of the kernel adapts locally to the geometry of the support. Moreover, they are nonnegative across the entire support of the target density, which sets them apart from many boundary bias-corrected estimators.

Negligible boundary bias is an inherent characteristic of asymmetric kernel smoothers, in contrast to other approaches such as the reflection method or boundary kernels; see, e.g., Schuster (1985), Müller (1991), and Jones (1993). This property makes them exceptionally user-friendly and among the simplest estimators to employ in the class of methods that feature asymptotic unbiasedness near the boundary. For an overview of the literature on asymmetric kernel estimators, refer to Hirukawa (2018) and Section 2 of Ouimet and Tolosana-Delgado (2022). For a review of associated kernels, which unify part of the theory for asymmetric kernels, see, e.g., Kokonendji and Somé (2018, 2021).

The asymptotic properties of the new MIG asymmetric kernel smoother  $\hat{f}_{n,\mathbf{H}}$  are stated in Section 5.1. Its finite-sample performance is then examined through simulation in Section 5.2. As an illustration of its practical utility, a bivariate version of  $\hat{f}_{n,\mathbf{H}}$  is used in Section 5.3 to smooth the posterior distribution of a generalized Pareto model fitted to large electromagnetic storms.

### 5.1. Asymptotic results

In this section, the local limit theorem for the MIG distribution given in Theorem 3.3 is used to derive the asymptotic variance of the new density estimator  $\hat{f}_{n,\mathbf{H}}$  at each point  $\boldsymbol{\xi}$  in the half-space  $\mathcal{H}_d(\boldsymbol{\beta})$ . The result, which is stated in Proposition 5.1, is complemented in Proposition 5.2 with a careful study of the asymptotic bias. This makes it possible to obtain the limiting forms of mean squared error and the mean integrated squared error of this estimator; see Corollaries 5.3 and 5.4, respectively. Moreover, the asymptotic normality of  $\hat{f}_{n,\mathbf{H}}$  at each point  $\boldsymbol{\xi}$  is provided in Theorem 5.5. The proofs are deferred to Appendix C.

Expectations are taken throughout with respect to the joint distribution of mutually independent copies  $\mathbf{X}_1, \dots, \mathbf{X}_n$  of  $\mathbf{X}$ . Whether explicitly or not, the bandwidth matrix parameter  $\mathbf{H} = \mathbf{H}(n)$  is assumed to be a function of the sample size whose spectral norm vanishes as  $n \rightarrow \infty$ , i.e.,  $\lim_{n \rightarrow \infty} \|\mathbf{H}\|_2 = 0$ .

**Proposition 5.1** (Pointwise variance). *Assume that  $f$  is Lipschitz continuous and bounded on the half-space  $\mathcal{H}_d(\boldsymbol{\beta})$ . Then, for any real vector  $\boldsymbol{\xi} \in \mathcal{H}_d(\boldsymbol{\beta})$ , one has, as  $n \rightarrow \infty$ ,*

$$\text{Var}\{\hat{f}_{n,\mathbf{H}}(\boldsymbol{\xi})\} = n^{-1}|\mathbf{H}|^{-1/2} \frac{f(\boldsymbol{\xi})}{(4\pi\boldsymbol{\beta}^\top \boldsymbol{\xi})^{d/2}} + o_{\boldsymbol{\beta},\boldsymbol{\xi}}(n^{-1}|\mathbf{H}|^{-1/2}),$$

where  $|\cdot|$  denotes the determinant.

**Proposition 5.2** (Pointwise bias). *Assume that  $f$  is twice differentiable, and its second order partial derivatives are uniformly continuous and bounded on the half-space  $\mathcal{H}_d(\beta)$ . Then, for any real vector  $\boldsymbol{\xi} \in \mathcal{H}_d(\beta)$ , one has, as  $n \rightarrow \infty$ ,*

$$\text{Bias}\{\hat{f}_{n,\mathbf{H}}(\boldsymbol{\xi})\} = \frac{1}{2}\boldsymbol{\beta}^\top \boldsymbol{\xi} \sum_{i,j=1}^d \mathbf{H}_{ij} \frac{\partial^2}{\partial \xi_i \partial \xi_j} f(\boldsymbol{\xi}) + o(\boldsymbol{\beta}^\top \boldsymbol{\xi} \|\mathbf{H}\|_2).$$

Alternatively, because the Hessian matrix  $D^2 f$  is symmetric, one can rewrite the above more compactly as

$$\text{Bias}\{\hat{f}_{n,\mathbf{H}}(\boldsymbol{\xi})\} = \frac{1}{2}\boldsymbol{\beta}^\top \boldsymbol{\xi} \text{tr}\{\mathbf{H}D^2 f(\boldsymbol{\xi})\} + o(\boldsymbol{\beta}^\top \boldsymbol{\xi} \|\mathbf{H}\|_2),$$

where  $\text{tr}(\cdot)$  denotes the trace.

As a corollary to Propositions 5.1–5.2, one obtains below the asymptotics of the mean squared error (MSE).

**Corollary 5.3** (Mean squared error). *Assume that  $f$  is twice differentiable, and its second order partial derivatives are uniformly continuous and bounded on the half-space  $\mathcal{H}_d(\beta)$ . Then, for any real vector  $\boldsymbol{\xi} \in \mathcal{H}_d(\beta)$ , one has, as  $n \rightarrow \infty$ ,*

$$\begin{aligned} \text{MSE}\{\hat{f}_{n,\mathbf{H}}(\boldsymbol{\xi})\} &= \mathbb{E}\left\{|\hat{f}_{n,\mathbf{H}}(\boldsymbol{\xi}) - f(\boldsymbol{\xi})|^2\right\} \\ &= n^{-1}|\mathbf{H}|^{-1/2} \frac{f(\boldsymbol{\xi})}{(4\pi\boldsymbol{\beta}^\top \boldsymbol{\xi})^{d/2}} + \frac{1}{4}(\boldsymbol{\beta}^\top \boldsymbol{\xi})^2 \text{tr}^2\{\mathbf{H}D^2 f(\boldsymbol{\xi})\} \\ &\quad + o_{\boldsymbol{\beta},\boldsymbol{\xi}}(n^{-1}|\mathbf{H}|^{-1/2}) + o\{(\boldsymbol{\beta}^\top \boldsymbol{\xi})^2 \|\mathbf{H}\|_2^2\}. \end{aligned}$$

The asymptotically optimal choice of  $\mathbf{H}$  with respect to MSE is

$$\mathbf{H}_{\text{opt}}(\boldsymbol{\xi}) = \underset{\mathbf{H} \in \mathcal{S}_{++}^d}{\text{argmin}} \left[ n^{-1}|\mathbf{H}|^{-1/2} \frac{f(\boldsymbol{\xi})}{(4\pi\boldsymbol{\beta}^\top \boldsymbol{\xi})^{d/2}} + \frac{1}{4}(\boldsymbol{\beta}^\top \boldsymbol{\xi})^2 \text{tr}^2\{\mathbf{H}D^2 f(\boldsymbol{\xi})\} \right].$$

If one restricts the bandwidth matrix  $\mathbf{H}$  to be a multiple of the identity matrix, viz.  $\mathbf{H} = h^2 \mathbf{I}_d$  for some real  $h \in (0, \infty)$ , then the asymptotically optimal choice of  $\mathbf{H}$  with respect to MSE is

$$\mathbf{H}_{\text{opt}}(\boldsymbol{\xi}) = \{h_{\text{opt}}(\boldsymbol{\xi})\}^2 \mathbf{I}_d,$$

where

$$h_{\text{opt}}(\boldsymbol{\xi}) = \left[ \frac{d}{n} \times \frac{f(\boldsymbol{\xi})/(4\pi\boldsymbol{\beta}^\top \boldsymbol{\xi})^{d/2}}{(\boldsymbol{\beta}^\top \boldsymbol{\xi})^2 \{\Delta f(\boldsymbol{\xi})\}^2} \right]^{1/(d+4)},$$

and where  $\Delta$  denotes the Laplacian operator. Consequently, one has, as  $n \rightarrow \infty$ ,

$$\begin{aligned} \text{MSE}\{\hat{f}_{n,\mathbf{H}_{\text{opt}}}(\boldsymbol{\xi})\} &= \frac{4+d}{4d} \left\{ \frac{d}{n} \times \frac{f(\boldsymbol{\xi})}{(4\pi\boldsymbol{\beta}^\top \boldsymbol{\xi})^{d/2}} \right\}^{4/(d+4)} \\ &\quad \times \left[ (\boldsymbol{\beta}^\top \boldsymbol{\xi})^2 \{\Delta f(\boldsymbol{\xi})\}^2 \right]^{d/(d+4)} + o(n^{-4/(d+4)}). \end{aligned}$$



Next, by integrating the MSE, one obtains the asymptotics of the mean integrated squared error.

**Corollary 5.4** (Mean integrated squared error). *Assume that  $f$  is twice differentiable and that its second order partial derivatives are uniformly continuous and bounded on the half-space  $\mathcal{H}_d(\boldsymbol{\beta})$ . Furthermore, assume that the target density  $f$  is such that the following integrals are finite:*

$$\int_{\mathcal{H}_d(\boldsymbol{\beta})} \frac{f(\boldsymbol{\xi})}{(4\pi\boldsymbol{\beta}^\top \boldsymbol{\xi})^{d/2}} d\boldsymbol{\xi} < \infty, \quad \int_{\mathcal{H}_d(\boldsymbol{\beta})} \frac{1}{4}(\boldsymbol{\beta}^\top \boldsymbol{\xi})^2 \text{tr}^2\{\mathbf{H}D^2 f(\boldsymbol{\xi})\} d\boldsymbol{\xi} < \infty.$$

Then, as  $n \rightarrow \infty$ , one has

$$\begin{aligned} \text{MISE}(\hat{f}_{n,\mathbf{H}}) &= n^{-1}|\mathbf{H}|^{-1/2} \int_{\mathcal{H}_d(\boldsymbol{\beta})} \frac{f(\boldsymbol{\xi})}{(4\pi\boldsymbol{\beta}^\top \boldsymbol{\xi})^{d/2}} d\boldsymbol{\xi} \\ &\quad + \int_{\mathcal{H}_d(\boldsymbol{\beta})} \frac{1}{4}(\boldsymbol{\beta}^\top \boldsymbol{\xi})^2 \text{tr}^2\{\mathbf{H}D^2 f(\boldsymbol{\xi})\} d\boldsymbol{\xi} \\ &\quad + o_{\boldsymbol{\beta}}(n^{-1}|\mathbf{H}|^{-1/2}) + o_{\boldsymbol{\beta}}(\|\mathbf{H}\|_2^2). \end{aligned}$$

The asymptotically optimal choice of  $\mathbf{H}$  with respect to MISE is

$$\begin{aligned} \mathbf{H}_{\text{opt}} = \underset{\mathbf{H} \in \mathcal{S}_{++}^d}{\text{argmin}} \left[ n^{-1}|\mathbf{H}|^{-1/2} \int_{\mathcal{H}_d(\boldsymbol{\beta})} \frac{f(\boldsymbol{\xi})}{(4\pi\boldsymbol{\beta}^\top \boldsymbol{\xi})^{d/2}} d\boldsymbol{\xi} \right. \\ \left. + \int_{\mathcal{H}_d(\boldsymbol{\beta})} \frac{1}{4}(\boldsymbol{\beta}^\top \boldsymbol{\xi})^2 \text{tr}^2\{\mathbf{H}D^2 f(\boldsymbol{\xi})\} d\boldsymbol{\xi} \right]. \end{aligned} \quad (5.2)$$

If one restricts the bandwidth matrix  $\mathbf{H}$  to be a multiple of the identity matrix, viz.  $\mathbf{H} = h^2 \mathbf{I}_d$  for some real  $h \in (0, \infty)$ , then the asymptotically optimal choice of  $\mathbf{H}$  with respect to MISE is

$$\mathbf{H}_{\text{opt}} = (h_{\text{opt}})^2 \mathbf{I}_d,$$

where

$$h_{\text{opt}} = \left[ \frac{d}{n} \times \frac{\int_{\mathcal{H}_d(\boldsymbol{\beta})} f(\boldsymbol{\xi}) / (4\pi\boldsymbol{\beta}^\top \boldsymbol{\xi})^{d/2} d\boldsymbol{\xi}}{\int_{\mathcal{H}_d(\boldsymbol{\beta})} (\boldsymbol{\beta}^\top \boldsymbol{\xi})^2 \{\Delta f(\boldsymbol{\xi})\}^2 d\boldsymbol{\xi}} \right]^{1/(d+4)}, \quad (5.3)$$

and where  $\Delta$  denotes the Laplacian operator. Consequently, one has, as  $n \rightarrow \infty$ ,

$$\begin{aligned} \text{MISE}(\hat{f}_{n,\mathbf{H}_{\text{opt}}}) &= \frac{4+d}{4d} \left\{ \frac{d}{n} \int_{\mathcal{H}_d(\boldsymbol{\beta})} \frac{f(\boldsymbol{\xi})}{(4\pi\boldsymbol{\beta}^\top \boldsymbol{\xi})^{d/2}} d\boldsymbol{\xi} \right\}^{4/(d+4)} \\ &\quad \times \left[ \int_{\mathcal{H}_d(\boldsymbol{\beta})} (\boldsymbol{\beta}^\top \boldsymbol{\xi})^2 \{\Delta f(\boldsymbol{\xi})\}^2 d\boldsymbol{\xi} \right]^{d/(d+4)} + o(n^{-4/(d+4)}). \end{aligned}$$

**Remark 5.1.** In both corollaries above, the asymptotically optimal bandwidth matrices depend on the unknown density  $f$ . These are called oracle bandwidths. In practice, one option is to replace  $f$  by the MIG density function  $k_{\beta, \xi_n^*, \Omega_n^*}$  to evaluate the expressions, where the parameter  $\beta \in \mathbb{R}^d$  is assumed to be known and the pair  $(\xi_n^*, \Omega_n^*)$  denotes the maximum likelihood estimator found in Appendix D.2 for the pair  $(\xi, \Omega)$ , or else the method-of-moment estimators. The integrals in (5.2) and (5.3) over the half-space  $\mathcal{H}_d(\beta)$  can then be estimated via Monte Carlo by drawing samples from the corresponding MIG distribution using the algorithm developed in Section 4. An alternative is to simulate instead data from a multivariate truncated Gaussian distribution, whose parameters match the sample mean and variance, over  $\{\mathbf{x} \in \mathbb{R}^d : \beta^\top \mathbf{x} > \delta\}$  for some buffer  $\delta \geq 0$ , or the multivariate truncated Gaussian maximum likelihood estimators (which requires numerical optimization). These are variations of the plug-in selection method; for alternatives, refer to Chapter 3 of Chacón and Duong (2018).

**Remark 5.2.** If margins have different scale parameters or exhibit correlations, using an isotropic model with bandwidth matrix  $\mathbf{H} = h^2 \mathbf{I}_d$  will be suboptimal. However, the data can be rotated, as proposed by Duong and Hazelton (2003), to work out the optimal bandwidth for  $\mathbf{X}^* = \mathbf{L}^{-1} \mathbf{X}$ , where  $\mathbf{L}^{-1}$  is the inverse of the lower triangular Cholesky root of the sample covariance matrix,  $\mathbf{S} = \mathbf{L} \mathbf{L}^\top$ . If  $\mathbf{X} \sim \text{MIG}(\beta, \xi, \Omega)$ , it is easy to see that  $\mathbf{L}^{-1} \mathbf{X} \sim \text{MIG}(\mathbf{L}^\top \beta, \mathbf{L}^{-1} \xi, \mathbf{L}^{-1} \Omega \mathbf{L}^{-\top})$  (Minami, 2003, Property 2), as the MIG family is closed under affine transformations. It follows that the data can first be rotated, an isotropic bandwidth can be estimated, and the latter can be back-transformed for smoothing the original data. Alternatively, scaling can be considered instead of rotation; for this, a similar procedure is followed by replacing  $\mathbf{S}$  with a diagonal matrix with the component-specific variances.

The asymptotic normality is obtained by a simple verification of the Lindeberg condition for double arrays.

**Theorem 5.5** (Asymptotic normality). *Assume that  $f$  is Lipschitz continuous and bounded on the half-space  $\mathcal{H}_d(\beta)$ . Let the real vector  $\xi \in \mathcal{H}_d(\beta)$  be such that  $f(\xi) \in (0, \infty)$ . If  $n^{1/2} |\mathbf{H}|^{1/4} \rightarrow \infty$  as  $n \rightarrow \infty$ , then*

$$n^{1/2} |\mathbf{H}|^{1/4} \left[ \hat{f}_{n, \mathbf{H}}(\xi) - \mathbb{E} \{ \hat{f}_{n, \mathbf{H}}(\xi) \} \right] \rightsquigarrow \mathcal{N}_d \left[ 0, \frac{f(\xi)}{(4\pi \beta^\top \xi)^{d/2}} \right].$$

*Alternatively, assume that  $f$  is twice differentiable and that its second order partial derivatives are uniformly continuous and bounded on the half-space  $\mathcal{H}_d(\beta)$ . If  $n^{1/2} |\mathbf{H}|^{1/4} \rightarrow \infty$  as  $n \rightarrow \infty$ , and if also  $n^{1/2} |\mathbf{H}|^{1/4} \|\mathbf{H}\|_2 \rightarrow 0$  as  $n \rightarrow \infty$ , then the last equation together with Proposition 5.2 imply*

$$n^{1/2} |\mathbf{H}|^{1/4} \{ \hat{f}_{n, \mathbf{H}}(\xi) - f(\xi) \} \rightsquigarrow \mathcal{N}_d \left[ 0, \frac{f(\xi)}{(4\pi \beta^\top \xi)^{d/2}} \right].$$

## 5.2. Simulation study

In this section, different choices of bandwidth for the MIG kernel smoother  $\hat{f}_{n,\mathbf{H}}$  are compared via simulation for a sample  $\mathbf{x}_1, \dots, \mathbf{x}_n$  over  $\mathcal{H}_d(\boldsymbol{\beta})$ . Among alternatives, bandwidth matrices that minimize the asymptotic MISE derived in Corollary 5.4 are considered, using the plug-in approach discussed in Remark 5.1 with either MIG or truncated Gaussian approximating densities. The second approach maximizes the leave-one-out likelihood cross-validation (LCV) score (Habbema, Hermans and van den Broek, 1974), viz.

$$\operatorname{argmax}_{\mathbf{H} \in \mathcal{S}_{++}^d} \frac{1}{n} \sum_{i=1}^n \ln \hat{f}_{n-1,\mathbf{H}}^{-(i)}(\mathbf{x}_i), \quad \hat{f}_{n-1,\mathbf{H}}^{-(i)}(\mathbf{x}_i) = \frac{1}{n-1} \sum_{\substack{j=1 \\ j \neq i}}^n k_{\boldsymbol{\beta}, \mathbf{x}_i, \mathbf{H}}(\mathbf{x}_j); \quad (5.4)$$

see, e.g., Section 2.1 of Zhang, King and Hyndman (2006). This method is sensitive to extremes and outliers, and can lead to oversmoothing when they are present. Other options include the least squares cross-validation criterion (Rudemo, 1982; Bowman, 1984), namely

$$\operatorname{argmax}_{\mathbf{H} \in \mathcal{S}_{++}^d} \left\{ \frac{1}{n} \sum_{i=1}^n \hat{f}_{n-1,\mathbf{H}}^{-(i)}(\mathbf{x}_i) - \frac{1}{2} \int_{\mathcal{H}_d(\boldsymbol{\beta})} \hat{f}_{n,\mathbf{H}}^2(\boldsymbol{\xi}) d\boldsymbol{\xi} \right\}, \quad (5.5)$$

and the robust LCV criterion of Wu (2019), which interpolates between the likelihood and least squares cross-validation. The integral in (5.5) can be evaluated via Monte Carlo, as discussed in Remark 5.1, or using a multivariate Laplace approximation.

With both asymptotic MISE and LCV, one can use a full  $d \times d$  bandwidth matrix and perform numerical optimization of the elements of the Cholesky root with positivity constraints for the diagonal (Pinheiro and Bates, 1996). Additionally, an isotropic bandwidth matrix of the form  $h^2 \mathbf{S}$  is considered, where  $h$  is obtained based on the transformed data as discussed in Remark 5.2. A diagonal bandwidth matrix  $\mathbf{H}_{nr}$  based on the ‘‘normal reference rule’’ is also tested, where the  $i$ th diagonal element is  $(\mathbf{H}_{nr})_{ii} = \hat{\sigma}_i [4/\{(d+2)n\}]^{1/(d+4)}$  for all  $i \in \{1, \dots, d\}$ ; see, e.g., Scott (2015, Eq. 6.43).

Let  $\mathbf{R}_d(\rho) = (1-\rho)\mathbf{I}_d + \rho\mathbf{1}_d\mathbf{1}_d^\top$  denote an equicorrelation matrix with correlation  $\rho \in (-1/(d-1), 1)$ , and let  $\boldsymbol{\nu}_d = (1, \dots, d)^\top$ . Different models over  $\mathcal{H}_d(\boldsymbol{\beta})$  are considered for  $\boldsymbol{\beta} = \mathbf{1}_d$  in dimension  $d \in \{2, 3, 4\}$ , with data drawn from

- $F_1$ : a Student- $t$  distribution truncated over  $\mathcal{H}_d(\boldsymbol{\beta})$ , with location vector  $\boldsymbol{\beta} + 0.1\mathbf{1}_d$ , scale matrix  $\operatorname{diag}(\sqrt{\boldsymbol{\nu}_d})\mathbf{R}_d(0.5)\operatorname{diag}(\sqrt{\boldsymbol{\nu}_d})$ , and  $\nu = 5$  degrees of freedom;
- $F_2$ : a two-component mixture distribution with weights (0.6, 0.4) following loosely the data generating mechanisms of Zhang, King and Hyndman (2006), where
  - a) the first component is a Student- $t$  distribution truncated over  $\mathcal{H}_d(\boldsymbol{\beta})$  with location vector  $\mathbf{1}_d$ , scale matrix  $\mathbf{R}_d(0.5)$ , and  $\nu = 5$  degrees of freedom;

b) the second component is a Gaussian distribution truncated over  $\mathcal{H}_d(\beta)$ , with location vector  $\beta + 10\mathbf{1}_d - \boldsymbol{\nu}_d$  and scale matrix  $\text{diag}(\boldsymbol{\nu}_d^{1/2})\mathbf{R}_d(-0.2)\text{diag}(\boldsymbol{\nu}_d^{1/2})$  over  $\mathcal{H}_d(\beta)$ ;

$F_3$ : a truncated multivariate skewed Gaussian distribution (Azzalini and Capitanio, 1999) with location vector  $\boldsymbol{\xi} = 4\mathbf{1}_d$ , scale matrix  $\boldsymbol{\Omega} = \text{diag}(\boldsymbol{\nu}_d^{1/2})\mathbf{R}_d(0.9)\text{diag}(\boldsymbol{\nu}_d^{1/2})$ , and slant parameter  $\boldsymbol{\alpha} = -5\mathbf{1}_d$ ;

$F_4$ : a MIG distribution with parameters  $\boldsymbol{\xi} = 2\mathbf{1}_d$  and  $\boldsymbol{\Omega} = \mathbf{R}_d(0.5)$ .

Figure 4 shows the log-density curves for the four data generating mechanisms in dimension  $d = 2$ . Distributions  $F_1$  and  $F_4$  have modes close to the boundary of the support.

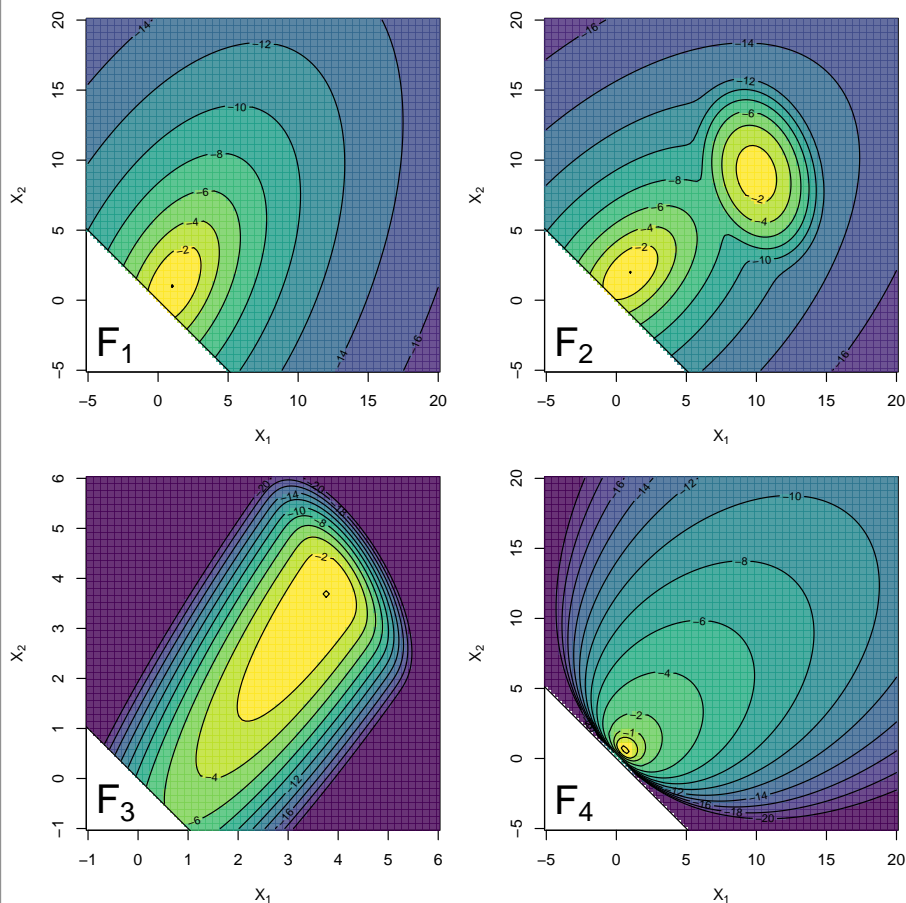


FIG 4. Log densities of the bivariate distributions  $F_1, \dots, F_4$ . The contour lines indicate differences in log density relative to the mode. Lighter colors (yellow) correspond to regions of higher density.

For each distribution  $F_1, \dots, F_4$ , samples of size  $n = 250$  and  $n = 500$  were simulated and the kernel density estimators were fitted with different bandwidth matrices, viz.

- $B_1$ : a full bandwidth matrix minimizing Eq. (5.2), with MIG plug-in for the density  $f$ ;
- $B_2$ : a full bandwidth matrix minimizing the LCV criterion of Eq. (5.4);
- $B_3$ : a spherical transformation and isotropic diagonal bandwidth matrix minimizing Eq. (5.3), with MIG plug-in for the density  $f$ ;
- $B_4$ : a spherical transformation and isotropic diagonal bandwidth matrix minimizing the LCV criterion of Eq. (5.4);
- $B_5$ : a spherical transformation and isotropic diagonal bandwidth matrix minimizing the robust LCV criterion (Wu, 2019);
- $B_6$ : a diagonal bandwidth using the normal reference rule.

Overall, for each dimension  $d \in \{2, 3, 4\}$ , target distribution  $F_i$  for  $i \in \{1, \dots, 4\}$ , sample size  $n \in \{250, 500\}$ , and bandwidth  $B_j$  with  $j \in \{1, \dots, 6\}$ , the root mean integrated squared error (RMISE),

$$\sqrt{\int_{\mathcal{H}_d(\beta)} \{\hat{f}_{n, B_j}(\mathbf{x}) - f_i(\mathbf{x})\}^2 d\mathbf{x}},$$

and the Kullback–Leibler divergence,

$$\int_{\mathcal{H}_d(\beta)} \{\ln \hat{f}_{n, B_j}(\mathbf{x}) - \ln f_i(\mathbf{x})\} f_i(\mathbf{x}) d\mathbf{x},$$

were estimated via Monte Carlo with  $10^4$  replications.

### 5.2.1. Results

The results of the simulation study are reported in Tables 1–2. The findings are briefly summarized below.

1. The methods giving the lowest average and median RMISE are the full bandwidth matrices minimizing the asymptotic RMISE ( $B_1$ ), which generally has the best performance, followed by the robust LCV criterion ( $B_5$ ). For the distribution  $F_4$ , the correct family  $f$  is used in (5.2), so the method  $B_1$  is expected to minimize RMISE in large samples.
2. Optimization of the isotropic model after performing a spherical transformation yields the worst performance across the board, then optimization of the full bandwidth matrix for both LCV ( $B_2$  versus  $B_4$ ) and asymptotic MISE approximations ( $B_1$  versus  $B_3$ ).
3. Optimization of the full covariance matrix with  $d(d-1)/2$  entries becomes increasing costly as the dimension grows. For example the median computing time for  $n = 500$  and  $d = 3$  for the full bandwidth minimizing the asymptotic RMISE,  $B_1$ , varies from 8.9 seconds ( $F_1$ ) to 21 seconds ( $F_4$ ).

TABLE 1

Estimated root mean integrated squared errors. Entries correspond to 1000 times the median (interquartile range) of  $10^3$  replications, as a function of the data generating distribution  $F \in \{F_1, \dots, F_4\}$ , the bandwidth  $B \in \{B_1, \dots, B_6\}$ , the sample size  $n \in \{250, 500\}$  and the dimension  $d \in \{2, 3, 4\}$ .

$F$	$B$	$d = 2$		$d = 3$		$d = 4$	
		$n = 250$	$n = 500$	$n = 250$	$n = 500$	$n = 250$	$n = 500$
$F_1$	$B_1$	25 (10)	22 (10)	12 (8)	11 (7)	4.3 (3.1)	3.9 (2.5)
	$B_2$	29 (14)	27 (18)	12 (11)	13 (13)	4.5 (5.2)	4.6 (5.1)
	$B_3$	29 (11)	27 (13)	12 (9)	13 (11)	4.0 (3.9)	4.3 (4.1)
	$B_4$	28 (11)	26 (14)	12 (10)	12 (11)	4.2 (3.9)	4.1 (4.0)
	$B_5$	25 (13)	22 (16)	12 (11)	12 (12)	4.5 (4.5)	4.2 (4.0)
	$B_6$	37 (7)	35 (8)	14 (4)	14 (5)	3.9 (1.4)	3.9 (1.7)
$F_2$	$B_1$	14 (4)	12 (3)	7 (2)	6 (1)	4.2 (0.5)	3.9 (0.4)
	$B_2$	36 (5)	36 (4)	8 (7)	7 (2)	4.5 (0.5)	4.3 (0.4)
	$B_3$	30 (4)	29 (3)	14 (1)	14 (1)	7.0 (0.1)	7.0 (0.1)
	$B_4$	17 (4)	15 (3)	8 (2)	7 (1)	4.8 (0.5)	4.4 (0.4)
	$B_5$	18 (4)	15 (3)	7 (2)	6 (1)	4.4 (0.6)	4.0 (0.5)
	$B_6$	39 (2)	38 (1)	17 (0)	17 (0)	7.4 (0.0)	7.4 (0.0)
$F_3$	$B_1$	59 (15)	49 (11)	39 (8)	34 (6)	22.1 (3.4)	19.6 (2.7)
	$B_2$	64 (16)	54 (13)	47 (8)	42 (6)	26.9 (3.2)	24.7 (2.4)
	$B_3$	135 (11)	129 (8)	87 (4)	84 (3)	44.0 (1.1)	43.1 (0.9)
	$B_4$	66 (17)	55 (13)	48 (8)	42 (6)	27.1 (3.3)	24.8 (2.4)
	$B_5$	59 (15)	48 (12)	44 (9)	39 (7)	25.8 (3.6)	23.6 (2.8)
	$B_6$	228 (3)	224 (2)	125 (1)	124 (0)	54.9 (0.2)	54.9 (0.2)
$F_4$	$B_1$	15 (5)	12 (4)	6 (2)	5 (1)	2.2 (0.5)	1.9 (0.4)
	$B_2$	22 (8)	17 (7)	9 (2)	8 (2)	3.4 (0.5)	3.1 (0.4)
	$B_3$	35 (5)	33 (4)	12 (1)	12 (1)	4.1 (0.3)	4.0 (0.2)
	$B_4$	25 (7)	21 (6)	11 (2)	10 (1)	3.8 (0.3)	3.6 (0.3)
	$B_5$	20 (6)	16 (5)	9 (2)	8 (1)	3.4 (0.4)	3.2 (0.3)
	$B_6$	43 (4)	41 (3)	14 (1)	14 (1)	4.6 (0.2)	4.5 (0.1)

TABLE 2  
 Estimated Kullback–Leibler divergences. Entries correspond to 100 times the median (interquartile range) of  $10^3$  replications, as a function of the data generating distribution  $F \in \{F_1, \dots, F_4\}$ , the bandwidth  $B \in \{B_1, \dots, B_6\}$ , the sample size  $n \in \{250, 500\}$  and the dimension  $d \in \{2, 3, 4\}$ .

$F$	$B$	$d = 2$		$d = 3$		$d = 4$	
		$n = 250$	$n = 500$	$n = 250$	$n = 500$	$n = 250$	$n = 500$
$F_1$	$B_1$	21 (6)	17 (4)	52 (9)	43 (6)	87 (11)	76 (7)
	$B_2$	9 (4)	6 (2)	20 (5)	15 (3)	32 (6)	26 (4)
	$B_3$	9 (3)	6 (2)	19 (4)	16 (3)	33 (6)	28 (4)
	$B_4$	9 (3)	6 (2)	19 (4)	15 (2)	32 (5)	26 (3)
	$B_5$	11 (4)	8 (2)	22 (5)	17 (3)	35 (5)	28 (3)
	$B_6$	15 (4)	12 (3)	39 (6)	35 (4)	72 (8)	66 (6)
$F_2$	$B_1$	22 (3)	17 (2)	41 (4)	35 (3)	62 (4)	54 (3)
	$B_2$	66 (18)	61 (13)	36 (58)	27 (4)	51 (6)	42 (3)
	$B_3$	74 (5)	70 (4)	106 (7)	103 (4)	149 (10)	145 (6)
	$B_4$	34 (5)	27 (4)	61 (4)	52 (3)	84 (4)	74 (3)
	$B_5$	37 (9)	29 (6)	64 (8)	54 (5)	86 (6)	76 (4)
	$B_6$	122 (6)	115 (3)	233 (6)	224 (4)	357 (8)	347 (5)
$F_3$	$B_1$	13 (3)	10 (2)	28 (4)	23 (3)	47 (5)	40 (3)
	$B_2$	14 (4)	10 (2)	26 (5)	20 (3)	39 (6)	31 (3)
	$B_3$	32 (4)	28 (3)	55 (5)	50 (4)	81 (7)	75 (5)
	$B_4$	13 (2)	10 (1)	24 (3)	20 (2)	35 (3)	30 (2)
	$B_5$	14 (5)	11 (3)	25 (3)	20 (2)	36 (4)	30 (2)
	$B_6$	117 (4)	110 (3)	228 (6)	218 (4)	347 (7)	334 (5)
$F_4$	$B_1$	11 (5)	7 (3)	26 (8)	18 (5)	47 (13)	33 (7)
	$B_2$	7 (3)	5 (2)	12 (4)	9 (2)	18 (5)	13 (3)
	$B_3$	8 (3)	7 (2)	14 (5)	11 (4)	21 (7)	18 (4)
	$B_4$	7 (2)	5 (2)	12 (4)	9 (2)	20 (5)	16 (3)
	$B_5$	8 (3)	5 (2)	15 (4)	11 (2)	24 (5)	19 (3)
	$B_6$	16 (5)	14 (3)	31 (7)	28 (5)	47 (10)	44 (7)

By contrast, the time it takes for the single parameter model minimizing the asymptotic RMISE is 0.03 seconds ( $F_1$ ) to 0.04 seconds ( $F_4$ ) for the spherical counterpart.

4. The most expensive methods are  $B_1$  and  $B_6$ , but the cost of leave-one-out cross-validation increases quadratically with the sample size  $n$ .
5. By nature, the LCV methods yield lower Kullback–Leibler divergence measures.
6. The LCV is more sensitive to extremes, particularly points lying close to the boundary and far from the mode. In some occurrences, this leads to drastic oversmoothing. The robust cross-validation criterion of Wu (2019) performs better but is more time-consuming, even in the isotropic setting ( $B_5$ ). The additional computational burden is due to the numerical evaluation of the integral defining the penalty.
7. All methods improve over the normal reference rule for both criteria.

**Remark 5.3.** The MIG distribution is more asymmetrical the closer the mode is to the boundary of  $\mathcal{H}_d(\beta)$ ; see the bottom right panel of Figure 4 for an illustration. This affects the properties of the kernel when the mode of the underlying process lies on the boundary. In such cases, using a truncated Gaussian or truncated Student- $t$  kernel, which could better accommodate such observations and outliers, would be preferable and might lead to lower RMISE values.

### 5.3. Real-data application

Data collected between 1957 and 2014 on the absolute magnitude of extreme geomagnetic storms lasting more than 48 hours, measured in disturbance-storm time (dst), are considered; see WDCG et al. (2015). A generalized Pareto distribution is fitted to exceedances above  $u = 220$  dst, with density given, for all  $x \in (0, \infty)$ , by

$$f(x) = \sigma_u^{-1} (1 + \xi x / \sigma_u)_+^{-1/\xi - 1}.$$

Coupled with a maximum data information prior,  $10^3$  draws from the posterior distribution of  $(\sigma_u, \xi)$  are obtained, supported on the (truncated) half-space

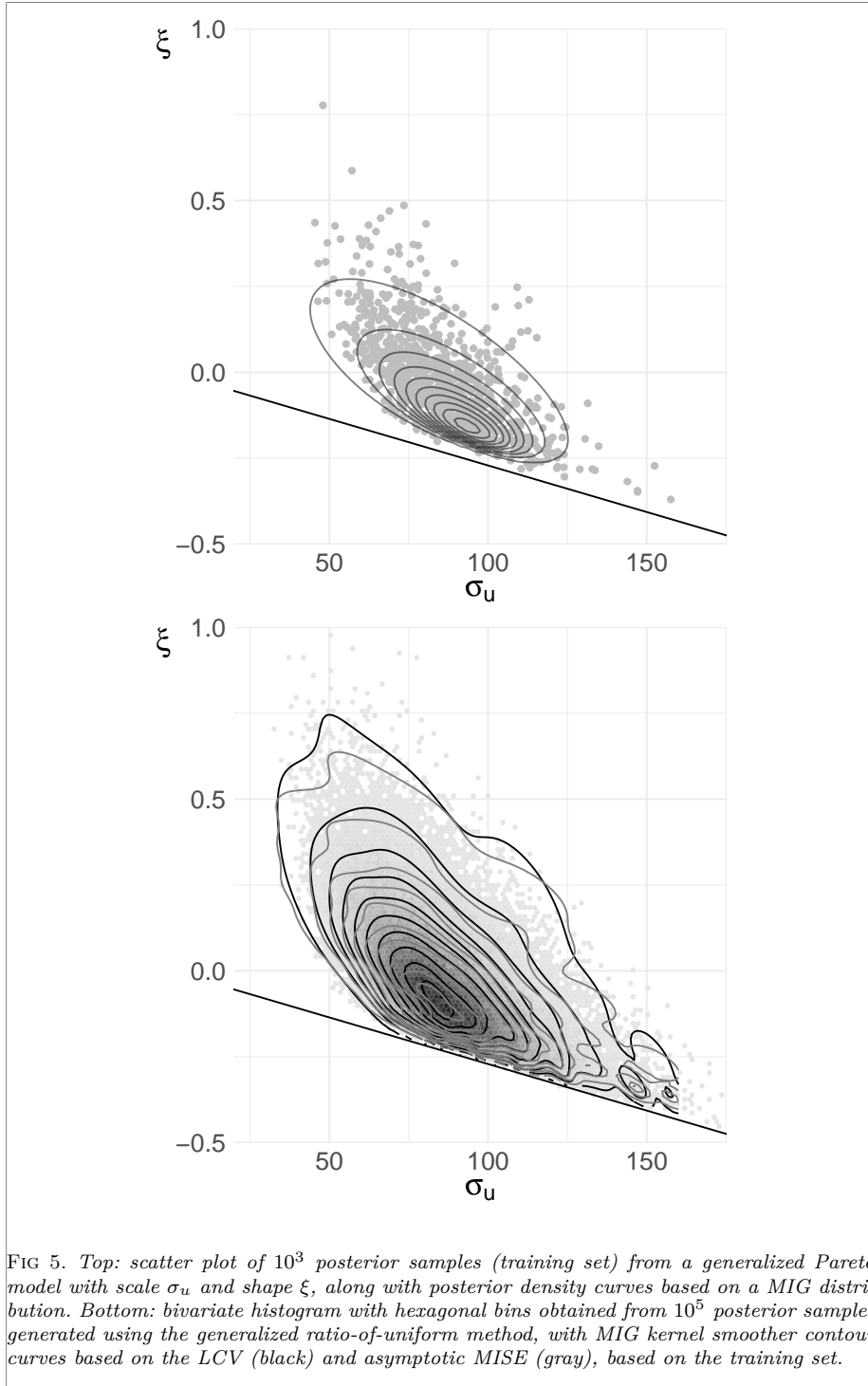
$$\mathcal{H}_2(1, m_n) = \{(\sigma_u, \xi) \in (0, \infty) \times \mathbb{R} : \sigma_u + \xi m_n > 0\}.$$

where  $m_n = \max(x_1, \dots, x_n)$ .

The top panel of Figure 5 shows the  $10^3$  posterior draws used for estimating the kernel density. Given the small sample size,  $n = 52$ , the posterior distribution of the generalized Pareto is far from Gaussian, notwithstanding the support constraint. The graph includes a scatterplot of the observations and contour curves for the MIG density evaluated at the maximum likelihood estimate.

The bottom panel of Figure 5 exhibits hexagonal bins of  $10^5$  data simulated from the posterior distribution, along with contour curves based on the training posterior draws. These curves were obtained by computing the full bandwidth matrix that minimizes the LCV (black) and the asymptotic MISE (gray) using





the MIG distribution to approximate the latter via Monte Carlo. Both bandwidths have correlations of roughly  $-2/3$ , which matches the sample correlation of the training set. However, the standard deviation in the shape direction ( $\xi$ ) for the LCV bandwidth is roughly twice that of the asymptotic MISE.

As one can see, the resulting density estimates faithfully reflect the repartition of the posterior draws. The MIG kernel density estimator is, by construction, more flexible than fixed parametric models such as the MIG distribution fitted in the top panel of Figure 5, with only a small cost. In more complex settings where exact sampling from the posterior is not available, kernel smoothing is a viable, cost-effective alternative that can lead to better approximations of the posterior density. While it is possible to use other smoothers, such as elliptical kernel smoothers truncated over the half-space, which can also generalize to include other linear inequality constraints, the MIG kernel does not require estimation of the normalizing constant and naturally adapts to the geometry of the half-space due to its asymmetry.

## Appendix A: Proofs of the normal approximations

### A.1. Proofs in the univariate case

#### A.1.1. Proof of Theorem 3.1

Let the positive reals  $\mu, \lambda \in (0, \infty)$  and  $x \in B_{\mu, \lambda}(\sqrt{\lambda/\mu})$  be given. Recall the definition of  $\delta_x$  in (3.4), and also

$$x \in B_{\mu, \lambda}(\sqrt{\lambda/\mu}) \quad \Rightarrow \quad |\delta_x| \sqrt{\frac{\mu}{\lambda}} < 1.$$

From the expression of the IG and Gaussian densities in (3.1) and (3.5), respectively, and using the decomposition

$$\frac{x}{\mu} = 1 + \delta_x \sqrt{\frac{\mu}{\lambda}},$$

one has

$$\begin{aligned} LR(x) &= \frac{3}{2} \ln \left( \frac{\mu}{x} \right) + \frac{(x - \mu)^2}{2\mu^3/\lambda} \left( 1 - \frac{\mu}{x} \right) \\ &= -\frac{3}{2} \ln \left( 1 + \delta_x \sqrt{\frac{\mu}{\lambda}} \right) + \frac{1}{2} \delta_x^2 \left\{ 1 - \left( 1 + \delta_x \sqrt{\frac{\mu}{\lambda}} \right)^{-1} \right\}. \end{aligned}$$

By applying the following Taylor expansions, valid for  $|y| < 1$ ,

$$-\ln(1 + y) = \sum_{k=1}^{\infty} \frac{(-1)^k}{k} y^k, \quad 1 - (1 + y)^{-1} = -\sum_{k=1}^{\infty} (-1)^k y^k, \quad (\text{A.1})$$

one obtains

$$\begin{aligned} LR(x) &= \frac{3}{2} \sum_{k=1}^{\infty} \frac{(-1)^k}{k} \left( \delta_x \sqrt{\frac{\mu}{\lambda}} \right)^k - \frac{1}{2} \delta_x^2 \sum_{k=1}^{\infty} (-1)^k \left( \delta_x \sqrt{\frac{\mu}{\lambda}} \right)^k \\ &= \sum_{k=1}^{\infty} (-1)^k \left( \frac{3}{2k} - \frac{\delta_x^2}{2} \right) \left( \delta_x \sqrt{\frac{\mu}{\lambda}} \right)^k, \end{aligned}$$

which proves (3.6).

One obtains (3.7) and (3.8) using the fact that the errors made when truncating the Taylor expansions in (A.1) are uniform on the compact set  $|y| \leq \tau \sqrt{\mu/\lambda}$  for any fixed real  $\tau \in (0, \sqrt{\lambda/\mu})$ . This concludes the proof.

#### A.1.2. Proof of Theorem 3.2

Given the relationships that exists between the different probability metrics in the statement of the theorem, see, e.g., [Gibbs and Su \(2002, p. 421\)](#), it is sufficient to prove the Hellinger distance bound.

Everywhere below, one writes  $B = \overline{B_{\mu,\lambda}}(0.5\sqrt{\lambda/\mu})$  for simplicity. Let  $X \sim \mathbb{P}_{\mu,\lambda}$ . By the bound on the squared Hellinger distance found at the bottom of p. 726 of [Carter \(2002\)](#), one knows that

$$H^2(\mathbb{P}_{\mu,\lambda}, \mathbb{Q}_{\mu,\lambda}) \leq 2\mathbb{P}(X \in B^c) + \mathbb{E} \left[ \ln \left\{ \frac{d\mathbb{P}_{\mu,\lambda}}{d\mathbb{Q}_{\mu,\lambda}}(X) \right\} \mathbf{1}_B(X) \right]. \quad (\text{A.2})$$

Then, by applying Chebyshev's inequality together with the fact that  $\text{Var}(\delta_X) = 1$  in (3.4), one has

$$\mathbb{P}(X \in B^c) = \mathbb{P} \left( |\delta_X| > 0.5\sqrt{\lambda/\mu} \right) \leq \frac{4\mu}{\lambda}. \quad (\text{A.3})$$

Also, by Theorem 3.1 and the identity  $\mathbf{1}_B = 1 - \mathbf{1}_{B^c}$ , one has

$$\begin{aligned} \mathbb{E} \left[ \ln \left\{ \frac{d\mathbb{P}_{\mu,\lambda}}{d\mathbb{Q}_{\mu,\lambda}}(X) \right\} \mathbf{1}_B(X) \right] &= \sqrt{\frac{\mu}{\lambda}} \mathbb{E} \left\{ \left( \frac{3\delta_X}{2} - \frac{\delta_X^3}{2} \right) \mathbf{1}_{B^c}(X) \right\} \\ &\quad - \sqrt{\frac{\mu}{\lambda}} \mathbb{E} \left( \frac{3\delta_X}{2} - \frac{\delta_X^3}{2} \right) + \mathcal{O}(\mu/\lambda). \end{aligned} \quad (\text{A.4})$$

The second term on the right-hand side of (A.4) is  $\mathcal{O}(\mu/\lambda)$  because  $\mathbb{E}(\delta_X) = 0$  by (3.2) and one knows that  $\mathbb{E}(\delta_X^3) = 3\sqrt{\mu/\lambda}$  from Section 15.4 of [Johnson, Kotz and Balakrishnan \(1994\)](#). The first term on the right-hand side of (A.4) is  $\mathcal{O}(\mu/\lambda)$  by Cauchy–Schwarz, (A.3), and the fact that all finite moments of  $\delta_X$  are  $\mathcal{O}(1)$  being asymptotically Gaussian. Indeed,

$$\begin{aligned} \left[ \mathbb{E} \left\{ \left( \frac{3\delta_X}{2} - \frac{\delta_X^3}{2} \right) \mathbf{1}_{B^c}(X) \right\} \right]^2 &\leq \mathbb{E} \left\{ \left( \frac{3\delta_X}{2} - \frac{\delta_X^3}{2} \right)^2 \right\} \times \mathbb{P}(X \in B^c) \\ &\leq \mathcal{O}(1) \times \frac{4\mu}{\lambda} = \mathcal{O}(\mu/\lambda). \end{aligned}$$

Therefore,

$$\mathbb{E} \left[ \ln \left\{ \frac{dP_{\mu,\lambda}}{dQ_{\mu,\lambda}}(X) \right\} \mathbf{1}_B(X) \right] = \mathcal{O}(\mu/\lambda). \quad (\text{A.5})$$

Combining the estimates (A.3) and (A.5) into (A.2) yields the conclusion that the squared Hellinger distance is of order  $\mathcal{O}(\mu/\lambda)$ , as claimed.

## A.2. Proofs in the multivariate case

### A.2.1. Proof of Theorem 3.3

Let the reals  $\mu, \omega \in (0, \infty)$ , and the real vectors  $\boldsymbol{\beta} \in \mathbb{R}^d$ ,  $\boldsymbol{\xi}_0 \in \mathcal{H}_d(\boldsymbol{\beta})$  and  $\mathbf{x} \in B_{\mu,\omega,\boldsymbol{\beta},\boldsymbol{\xi}_0,\boldsymbol{\Omega}_0}(\sqrt{\mu/\omega})$  be given. Recall the definition of  $\boldsymbol{\delta}_\mathbf{x}$  in (3.13), and also

$$\mathbf{x} \in B_{\mu,\omega,\boldsymbol{\beta},\boldsymbol{\xi}_0,\boldsymbol{\Omega}_0}(\sqrt{\mu/\omega}) \quad \Rightarrow \quad \frac{|\boldsymbol{\beta}^\top \boldsymbol{\Omega}_0^{1/2} \boldsymbol{\delta}_\mathbf{x}|}{\sqrt{\boldsymbol{\beta}^\top \boldsymbol{\xi}_0}} \sqrt{\frac{\omega}{\mu}} < 1.$$

From the expressions of the MIG and multivariate Gaussian densities in (3.11) and (3.14) respectively, and using the decomposition

$$\frac{\boldsymbol{\beta}^\top \mathbf{x}}{\mu \boldsymbol{\beta}^\top \boldsymbol{\xi}_0} = 1 + \frac{\boldsymbol{\beta}^\top \boldsymbol{\Omega}_0^{1/2} \boldsymbol{\delta}_\mathbf{x}}{\sqrt{\boldsymbol{\beta}^\top \boldsymbol{\xi}_0}} \sqrt{\frac{\omega}{\mu}},$$

one has

$$\begin{aligned} LR(\mathbf{x}) &= \left( \frac{d}{2} + 1 \right) \ln \left( \frac{\mu \boldsymbol{\beta}^\top \boldsymbol{\xi}_0}{\boldsymbol{\beta}^\top \mathbf{x}} \right) \\ &\quad + \frac{1}{2} (\mathbf{x} - \mu \boldsymbol{\xi}_0)^\top (\mu \omega \boldsymbol{\beta}^\top \boldsymbol{\xi}_0)^{-1} \boldsymbol{\Omega}_0^{-1} (\mathbf{x} - \mu \boldsymbol{\xi}_0) \left( 1 - \frac{\mu \boldsymbol{\beta}^\top \boldsymbol{\xi}_0}{\boldsymbol{\beta}^\top \mathbf{x}} \right) \\ &= - \left( \frac{d}{2} + 1 \right) \ln \left( 1 + \frac{\boldsymbol{\beta}^\top \boldsymbol{\Omega}_0^{1/2} \boldsymbol{\delta}_\mathbf{x}}{\sqrt{\boldsymbol{\beta}^\top \boldsymbol{\xi}_0}} \sqrt{\frac{\omega}{\mu}} \right) \\ &\quad + \frac{1}{2} \boldsymbol{\delta}_\mathbf{x}^\top \boldsymbol{\delta}_\mathbf{x} \left\{ 1 - \left( 1 + \frac{\boldsymbol{\beta}^\top \boldsymbol{\Omega}_0^{1/2} \boldsymbol{\delta}_\mathbf{x}}{\sqrt{\boldsymbol{\beta}^\top \boldsymbol{\xi}_0}} \sqrt{\frac{\omega}{\mu}} \right)^{-1} \right\}. \end{aligned}$$

By applying the following Taylor expansions, valid for  $|y| < 1$ ,

$$-\ln(1+y) = \sum_{k=1}^{\infty} \frac{(-1)^k}{k} y^k, \quad 1 - (1+y)^{-1} = - \sum_{k=1}^{\infty} (-1)^k y^k, \quad (\text{A.6})$$

one obtains

$$\begin{aligned} LR(\mathbf{x}) &= \left(\frac{d}{2} + 1\right) \sum_{k=1}^{\infty} \frac{(-1)^k}{k} \left( \frac{\boldsymbol{\beta}^\top \boldsymbol{\Omega}_0^{1/2} \boldsymbol{\delta}_\mathbf{x}}{\sqrt{\boldsymbol{\beta}^\top \boldsymbol{\xi}_0}} \sqrt{\frac{\omega}{\mu}} \right)^k \\ &\quad - \frac{1}{2} \boldsymbol{\delta}_\mathbf{x}^\top \boldsymbol{\delta}_\mathbf{x} \sum_{k=1}^{\infty} (-1)^k \left( \frac{\boldsymbol{\beta}^\top \boldsymbol{\Omega}_0^{1/2} \boldsymbol{\delta}_\mathbf{x}}{\sqrt{\boldsymbol{\beta}^\top \boldsymbol{\xi}_0}} \sqrt{\frac{\omega}{\mu}} \right)^k \\ &= \sum_{k=1}^{\infty} (-1)^k \left( \frac{d+2}{2k} - \frac{\boldsymbol{\delta}_\mathbf{x}^\top \boldsymbol{\delta}_\mathbf{x}}{2} \right) \left( \frac{\boldsymbol{\beta}^\top \boldsymbol{\Omega}_0^{1/2} \boldsymbol{\delta}_\mathbf{x}}{\sqrt{\boldsymbol{\beta}^\top \boldsymbol{\xi}_0}} \sqrt{\frac{\omega}{\mu}} \right)^k, \end{aligned}$$

which proves (3.15).

One obtains (3.16) and (3.17) using the fact that the errors made when truncating the Taylor expansions in (A.6) are uniform on the compact set  $|y| \leq \tau \sqrt{\omega/\mu}$  for any fixed real  $\tau \in (0, \sqrt{\mu/\omega})$ . This concludes the proof.

#### A.2.2. Proof of Theorem 3.4

Given the relationship there exists between the different probability metrics in the statement of the theorem, see, e.g., Gibbs and Su (2002, p. 421), it is sufficient to prove the Hellinger distance bound.

Everywhere below, one writes  $B = B_{\mu, \omega, \boldsymbol{\beta}, \boldsymbol{\xi}_0, \boldsymbol{\Omega}_0}(0.5\sqrt{\mu/\omega})$  for simplicity. Let  $\mathbf{X} \sim \mathbb{P}_{\mu, \omega, \boldsymbol{\beta}, \boldsymbol{\xi}_0, \boldsymbol{\Omega}_0}$ . By the bound on the squared Hellinger distance found at the bottom of p. 726 of Carter (2002), one knows that

$$\begin{aligned} &\mathbf{H}^2(\mathbb{P}_{\mu, \omega, \boldsymbol{\beta}, \boldsymbol{\xi}_0, \boldsymbol{\Omega}_0}, \mathbb{Q}_{\mu, \omega, \boldsymbol{\beta}, \boldsymbol{\xi}_0, \boldsymbol{\Omega}_0}) \\ &\leq 2 \mathbb{P}(\mathbf{X} \in B^c) + \mathbb{E} \left[ \ln \left\{ \frac{d\mathbb{P}_{\mu, \omega, \boldsymbol{\beta}, \boldsymbol{\xi}_0, \boldsymbol{\Omega}_0}(\mathbf{X})}{d\mathbb{Q}_{\mu, \omega, \boldsymbol{\beta}, \boldsymbol{\xi}_0, \boldsymbol{\Omega}_0}} \right\} \mathbb{1}_B(\mathbf{X}) \right]. \end{aligned} \quad (\text{A.7})$$

By a union bound on the summands of the quantity  $\boldsymbol{\beta}^\top \boldsymbol{\Omega}_0 \boldsymbol{\delta}_\mathbf{x}$ , followed by an application of Chebyshev's inequality for each summand and the exploitation of the fact that the margins of the MIG distribution are asymptotically Gaussian with mean  $\mu \xi_{0,j}$  and variance proportional to  $\mu \omega$  by (3.13), one has

$$\begin{aligned} &\mathbb{P}(\mathbf{X} \in B^c) \\ &= \mathbb{P} \left( \left| \boldsymbol{\beta}^\top \boldsymbol{\Omega}_0 \boldsymbol{\delta}_\mathbf{x} \right| > 0.5 \sqrt{\frac{\mu}{\omega}} \sqrt{\boldsymbol{\beta}^\top \boldsymbol{\xi}_0} \right) \\ &\leq \sum_{i=1}^d \mathbb{P} \left\{ \left| (\boldsymbol{\beta}^\top \boldsymbol{\Omega}_0)_i (\boldsymbol{\delta}_\mathbf{x})_i \right| > \frac{0.5}{d} \sqrt{\frac{\mu}{\omega}} \sqrt{\boldsymbol{\beta}^\top \boldsymbol{\xi}_0} \right\} \\ &\leq \sum_{i=1}^d \sum_{j=1}^d \mathbb{P} \left\{ \left| (\boldsymbol{\beta}^\top \boldsymbol{\Omega}_0)_i (\boldsymbol{\Omega}_0^{-1/2})_{ij} \frac{(X_j - \mu \xi_{0,j})}{\sqrt{\mu \omega \boldsymbol{\beta}^\top \boldsymbol{\xi}_0}} \right| > \frac{0.5}{d^2} \sqrt{\frac{\mu}{\omega}} \sqrt{\boldsymbol{\beta}^\top \boldsymbol{\xi}_0} \right\} \\ &= \mathcal{O}_{\boldsymbol{\beta}, \boldsymbol{\xi}_0, \boldsymbol{\Omega}_0}(\omega/\mu). \end{aligned} \quad (\text{A.8})$$

Also, by Theorem 3.3 and the identity  $\mathbb{1}_B = 1 - \mathbb{1}_{B^c}$ , one has

$$\begin{aligned} & \mathbb{E} \left[ \ln \left\{ \frac{dP_{\mu, \omega, \beta, \xi_0, \Omega_0}}{dQ_{\mu, \omega, \beta, \xi_0, \Omega_0}}(\mathbf{X}) \right\} \mathbb{1}_B(\mathbf{X}) \right] \\ &= \sqrt{\frac{\omega}{\mu}} \frac{\beta^\top \Omega_0^{1/2}}{\sqrt{\beta^\top \xi_0}} \mathbb{E} \left[ \left\{ \frac{(d+2)\delta_{\mathbf{X}}}{2} - \frac{\delta_{\mathbf{X}} \delta_{\mathbf{X}}^\top \delta_{\mathbf{X}}}{2} \right\} \mathbb{1}_{B^c}(\mathbf{X}) \right] \\ &\quad - \sqrt{\frac{\omega}{\mu}} \frac{\beta^\top \Omega_0^{1/2}}{\sqrt{\beta^\top \xi_0}} \mathbb{E} \left[ \left\{ \frac{(d+2)\delta_{\mathbf{X}}}{2} - \frac{\delta_{\mathbf{X}} \delta_{\mathbf{X}}^\top \delta_{\mathbf{X}}}{2} \right\} \right] \\ &\quad + \mathcal{O}_{\beta, \xi_0, \Omega_0}(\omega/\mu). \end{aligned} \tag{A.9}$$

The second term on the right-hand side of (A.9) is  $\mathcal{O}_{\beta, \xi_0, \Omega_0}(\omega/\mu)$  because  $\mathbb{E}(\delta_{\mathbf{X}}) = \mathbf{0}_d$  by (3.12), and using the fact that  $\mathbb{E}(\delta_{x,i} \delta_{x,j} \delta_{x,k}) = \mathcal{O}_{\beta, \xi_0, \Omega_0}(\sqrt{\omega/\mu})$  for all  $i, j, k \in \{1, \dots, d\}$ , which can be deduced from Property 1 of Minami (2003). The first term on the right-hand side of (A.9) is  $\mathcal{O}_{\beta, \xi_0, \Omega_0}(\omega/\mu)$  by Cauchy–Schwarz, Eq. (A.8) and the fact that all finite joint moments of the components of  $\delta_{\mathbf{X}}$  are  $\mathcal{O}_{\beta, \xi_0, \Omega_0}(1)$  being asymptotically Gaussian. Indeed,

$$\begin{aligned} & \left( \mathbb{E} \left[ \left\{ \frac{(d+2)\delta_{\mathbf{X}}}{2} - \frac{\delta_{\mathbf{X}} \delta_{\mathbf{X}}^\top \delta_{\mathbf{X}}}{2} \right\} \mathbb{1}_{B^c}(\mathbf{X}) \right] \right)^2 \\ & \leq \mathbb{E} \left[ \left\{ \frac{(d+2)\delta_{\mathbf{X}}}{2} - \frac{\delta_{\mathbf{X}} \delta_{\mathbf{X}}^\top \delta_{\mathbf{X}}}{2} \right\}^2 \right] \times \mathbb{P}(\mathbf{X} \in B^c) \\ & = \mathcal{O}_{\beta, \xi_0, \Omega_0}(1) \times \mathcal{O}_{\beta, \xi_0, \Omega_0}(\omega/\mu) \\ & = \mathcal{O}_{\beta, \xi_0, \Omega_0}(\omega/\mu). \end{aligned}$$

Therefore,

$$\mathbb{E} \left[ \ln \left\{ \frac{dP_{\mu, \omega, \beta, \xi_0, \Omega_0}}{dQ_{\mu, \omega, \beta, \xi_0, \Omega_0}}(\mathbf{X}) \right\} \mathbb{1}_B(\mathbf{X}) \right] = \mathcal{O}_{\beta, \xi_0, \Omega_0}(\omega/\mu). \tag{A.10}$$

Combining the estimates from (A.8) and (A.10) into (A.7) yields the conclusion that the squared Hellinger distance is of order  $\mathcal{O}_{\beta, \xi_0, \Omega_0}(\omega/\mu)$ , as claimed.

## Appendix B: Distribution function evaluation for MIG vectors

In this section, the stochastic representation in Proposition 4.1 is leveraged to evaluate the distribution function of a  $d$ -variate MIG vector,  $\mathbf{X} \sim \text{MIG}(\beta, \xi, \Omega)$ .

### B.1. General strategy

Let  $f_R(\cdot) \equiv k_{\beta^\top \xi, (\beta^\top \xi)^2 / (\beta^\top \Omega \beta)}(\cdot)$  and  $F_R$  denote the density and distribution function, respectively, of the univariate inverse Gaussian random variable  $R$  given in (4.1). By Proposition 4.1, the distribution function of  $\mathbf{X} \sim$

MIG( $\boldsymbol{\beta}, \boldsymbol{\xi}, \boldsymbol{\Omega}$ ) can be written, at any  $\mathbf{q} \in \mathbb{R}^d$ , as

$$\begin{aligned} \Pr(\mathbf{X} \leq \mathbf{q}) &= \int_{r_{\min}}^{r_{\max}} \int_{\mathbb{R}^{d-1}} \mathbb{1}_{[\mathbf{z}_{\min}(r), \mathbf{z}_{\max}(r)]}(\mathbf{z}) \phi_{d-1}\{\mathbf{z}; \boldsymbol{\mu}(r), r\boldsymbol{\Sigma}\} f_R(r) d\mathbf{z} dr, \end{aligned} \quad (\text{B.1})$$

where  $\boldsymbol{\mu}(\cdot)$  and  $\boldsymbol{\Sigma}$  are given in (4.2),

$$r_{\min} = \max\left(0, \min_{\mathbf{x} \in (-\infty_d, \mathbf{q}]} \boldsymbol{\beta}^\top \mathbf{x}\right), \quad r_{\max} = \max\left(0, \max_{\mathbf{x} \in (-\infty_d, \mathbf{q}]} \boldsymbol{\beta}^\top \mathbf{x}\right),$$

with  $-\infty_d = (-\infty, \dots, -\infty)^\top$ , and  $\phi_k(\cdot; \mathbf{m}, \mathbf{C})$  is the density function of a  $k$ -dimensional Gaussian vector with mean  $\mathbf{m}$  and covariance matrix  $\mathbf{C}$ . Derivation of the integration bounds for  $R$  and  $\mathbf{Z} \mid R = r$  requires some work, as the region of integration is a rotated polytope.

Given that  $\mathbf{Z} \mid R = r$  is a location and scale mixture of Gaussian vectors, separation-of-variables (Genz and Bretz, 2009) can be used to evaluate the innermost Gaussian integral in (B.1). Let  $\mathbf{L}$  denote the lower triangular Cholesky root of the covariance matrix  $\boldsymbol{\Sigma} = \mathbf{L}\mathbf{L}^\top$ , and let  $\mathbf{Y} \sim \mathcal{N}_{d-1}(\mathbf{0}_{d-1}, \mathbf{I}_{d-1})$  be a standard Gaussian vector. The triangular system of equations leads to a sequential decomposition of the region of integration as follows:

$$\Pr(\mathbf{Z} \leq \mathbf{z} \mid R = r) = \int_{a_1}^{b_1} \cdots \int_{a_{d-1}}^{b_{d-1}} \phi_{d-1}(\mathbf{y}; \mathbf{0}_{d-1}, \mathbf{I}_{d-1}) d\mathbf{y},$$

where

$$\begin{aligned} a_1 &= L_{11}^{-1} r^{-1/2} \{z_{\min,1}(r) - \mu_1(r)\}, \\ b_1 &= L_{11}^{-1} r^{-1/2} \{z_{\max,1}(r) - \mu_1(r)\}, \end{aligned}$$

and, for every  $j \in \{2, \dots, d-1\}$ ,

$$\begin{aligned} a_j &= \frac{r^{-1/2} \{z_{\min,j}(r, z_1, \dots, z_{j-1}) - \mu_j(r)\} - \sum_{i=1}^{j-1} L_{ji} y_i}{L_{jj}}, \\ b_j &= \frac{r^{-1/2} \{z_{\max,j}(r, z_1, \dots, z_{j-1}) - \mu_j(r)\} - \sum_{i=1}^{j-1} L_{ji} y_i}{L_{jj}}. \end{aligned}$$

This suggests that a sensible Monte Carlo estimator can be obtained by sequential importance sampling using

$$\begin{aligned} g_{\text{sov}}(r, \mathbf{y}) &= \frac{f_R(r)}{F_R(r)} f(y_1 \mid r) \prod_{j=2}^{d-1} f(y_j \mid r, y_1, \dots, y_{j-1}) \\ &= \frac{f_R(r)}{F_R(r)} \prod_{j=1}^{d-1} \frac{\phi(y_j) \mathbb{1}_{[a_j, b_j]}(y_j)}{\Phi(b_j) - \Phi(a_j)} \end{aligned}$$

as the importance sampling density, where  $\phi$  and  $\Phi$  denote the univariate standard normal density and distribution function, respectively. Univariate draws

from the truncated inverse Gaussian distribution can be obtained using rejection sampling. Based on  $T$  draws from the distribution function associated to  $g_{\text{sov}}$ , the separation-of-variable estimator of the integral in (B.1) is

$$F_R(r) \times \frac{1}{T} \sum_{t=1}^T \prod_{j=1}^{d-1} \{\Phi(b_j^{(t)}) - \Phi(a_j^{(t)})\}. \quad (\text{B.2})$$

The separation-of-variables algorithm is described on p. 50 of [Genz and Bretz \(2009\)](#) using a randomized quasi Monte Carlo procedure; see also [Hintz, Hofert and Lemieux \(2021\)](#), who discuss alternative quasi Monte Carlo schemes and reordering strategies for scale mixtures.

### B.2. Integration bounds in dimension $d = 2$

It is instructive to consider first the bivariate case. Given  $\boldsymbol{\beta} = (\beta_1, \beta_2)^\top \in \mathbb{R}^2$ , denote the radius  $R = \boldsymbol{\beta}^\top \mathbf{X} \in (0, \infty)$ . Take  $\mathbf{Q}_2 = (-\beta_2, \beta_1)/|\boldsymbol{\beta}|_2$  to be a vector of unit length orthogonal to  $\boldsymbol{\beta}$ .

The probability of falling in  $(-\infty_2, \mathbf{q}]$  is

$$\Pr(\mathbf{X} \leq \mathbf{q}) = \int_{r_{\min}}^{r_{\max}} \Pr\{z_{\min}(r) \leq Z \leq z_{\max}(r) \mid R = r\} f_R(r) dr.$$

Figure 6 illustrates how the region of integration changes, depending on the position of  $(-\infty_2, \mathbf{q}]$  with respect to the half-space  $\mathcal{H}_2(\boldsymbol{\beta})$ . First, obtain the coordinates of the vertices defining the region of integration,  $(-\infty_2, \mathbf{q}] \cap \mathcal{H}_2(\boldsymbol{\beta})$ . For each of these vertices, apply the linear transformation  $\mathbf{Q}_2$  and observe where these points are mapped to get integration bounds for  $R$  and  $Z \mid R$ .

Let  $\mathbf{e}_1 = (1, 0)^\top$  and  $\mathbf{e}_2 = (0, 1)^\top$  be the two standard unit vectors in  $\mathbb{R}^2$ . A careful case-by-case analysis leads to the following integration bounds:

1. If  $\beta_1 > 0, \beta_2 > 0$ , then  $\Pr(\mathbf{X} \leq \mathbf{q}) = 0$  if  $\boldsymbol{\beta}^\top \mathbf{q} \leq 0$ . Otherwise, the vertices of the triangle defining the region of integration are  $\{\mathbf{q}, \mathbf{v}_1 = (q_1, -\beta_1 q_1/\beta_2), \mathbf{v}_2 = (-\beta_2 q_2/\beta_1, q_2)\}$ . In the transformed space, the region of integration is a rotated triangle which goes from  $r = 0$ , with  $z_{\min}(0) = \mathbf{Q}_2 \mathbf{v}_1$  and  $z_{\max}(0) = \mathbf{Q}_2 \mathbf{v}_2$ , to  $r_{\max} = \boldsymbol{\beta}^\top \mathbf{q}$ , with

$$\begin{aligned} z_{\min}(r) &= \{r/(\boldsymbol{\beta}^\top \mathbf{e}_2)\} \mathbf{Q}_2 \mathbf{e}_2 + z_{\min}(0), \\ z_{\max}(r) &= \{r/(\boldsymbol{\beta}^\top \mathbf{e}_1)\} \mathbf{Q}_2 \mathbf{e}_1 + z_{\max}(0). \end{aligned}$$

2. If  $\beta_1 < 0$  and  $\beta_2 > 0$ , there are two cases. If  $\mathbf{q} \notin \mathcal{H}_2(\boldsymbol{\beta})$ , then the region of integration is a triangle, and so is its transformed counterpart. The bounds go from  $r_{\min} = 0$  to  $r_{\max} = \infty$ , with  $z_{\min}(r) = \boldsymbol{\beta}^\top \mathbf{q} - (r/\beta_1) \mathbf{Q}_2 \mathbf{e}_1$ . If  $\mathbf{q} \in \mathcal{H}_2(\boldsymbol{\beta})$ , then  $R$  ranges from  $r_{\min} = \boldsymbol{\beta}^\top \mathbf{q}$  to  $r_{\max} = \infty$ , while

$$\begin{aligned} z_{\min}(r) &= \max\{\mathbf{Q}_2 \mathbf{v}_2 + (r/\beta_1) \mathbf{Q}_2 \mathbf{e}_1, \mathbf{Q}_2 \mathbf{v}_1 + (r/\beta_2) \mathbf{Q}_2 \mathbf{e}_2\}, \\ z_{\max}(r) &= \infty. \end{aligned}$$



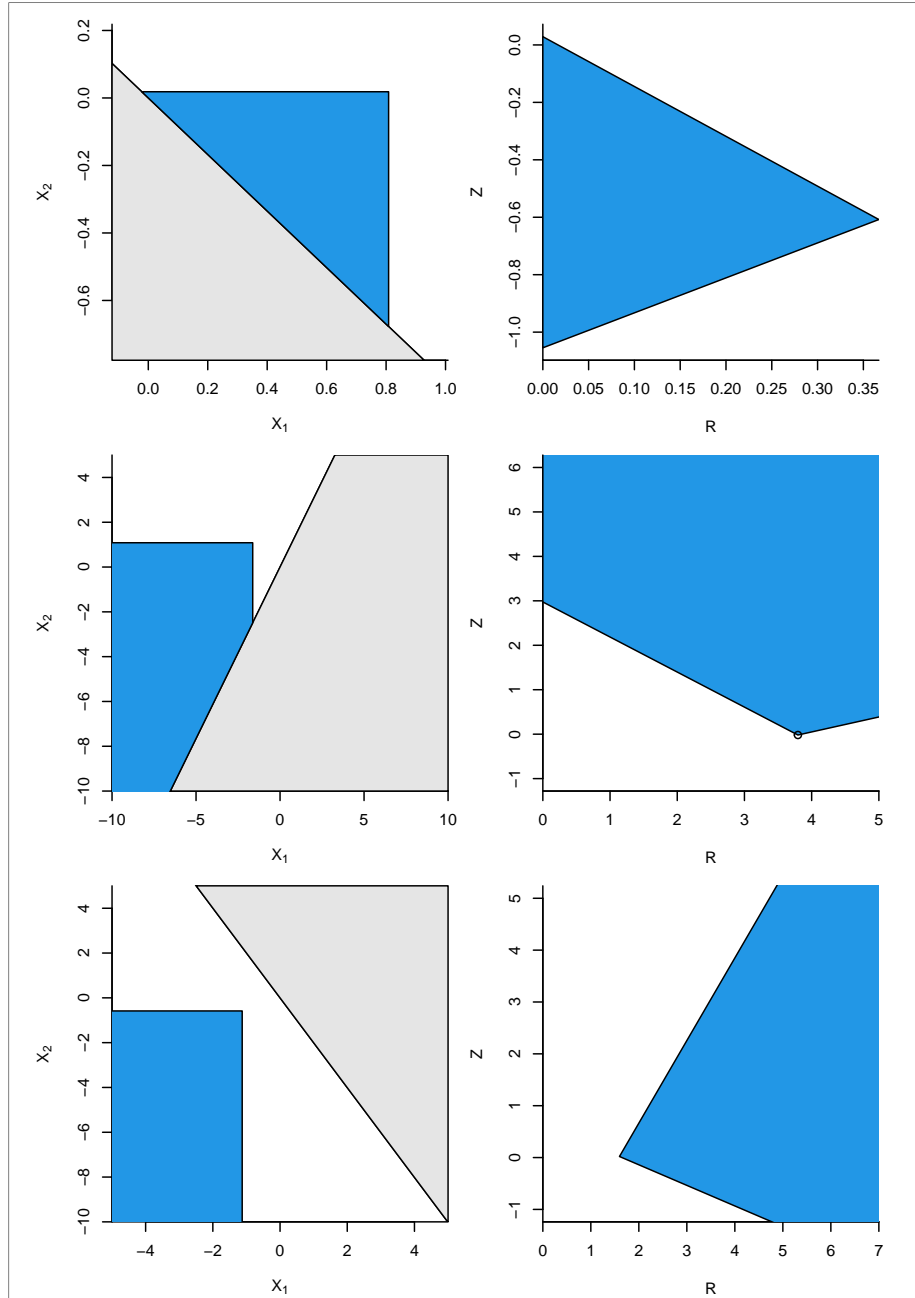


FIG 6. Changes in the region of integration induced by the linear transformation  $\mathbf{Q}$  from the original space  $(-\infty_2, \mathbf{q}] \cap \mathcal{H}_2(\beta)$  (left) to  $\mathbf{Q}\{(-\infty_2, \mathbf{q}] \cap \mathcal{H}_2(\beta)\}$  (right) for different combinations of  $\beta$  with  $\beta_1 > 0, \beta_2 > 0$  (top),  $\beta_1 < 0, \beta_2 > 0$  (middle) and  $\beta_1 < 0, \beta_2 < 0$  (bottom). The shaded grey regions in the left panels indicate values outside of the support of the distribution.

3. If  $\beta_1 > 0$  and  $\beta_2 < 0$ , then  $R$  ranges from  $r_{\min} = 0$  to  $r_{\max} = \infty$ , and

$$\begin{aligned} z_{\min}(r) &= -\infty, \\ z_{\max}(r) &= \min\{\mathbf{Q}_2\mathbf{v}_2 + (r/\beta_1)\mathbf{Q}_2\mathbf{e}_1, \mathbf{Q}_2\mathbf{v}_1 + (r/\beta_2)\mathbf{Q}_2\mathbf{e}_2\}. \end{aligned}$$

4. If  $\beta_1 < 0$  and  $\beta_2 < 0$ , then the integration goes from  $r_{\min} = \max(0, \beta^\top \mathbf{q})$  to  $r_{\max} = \infty$ , where

$$\begin{aligned} z_{\min}(r) &= \mathbf{Q}_2\mathbf{v}_2 + (r/\beta_1)\mathbf{Q}_2\mathbf{e}_1, \\ z_{\max}(r) &= \mathbf{Q}_2\mathbf{v}_1 + (r/\beta_2)\mathbf{Q}_2\mathbf{e}_2. \end{aligned}$$

5. If  $\beta_1 = 0$ , then  $r_{\min} = 0$  and  $r_{\max} = \beta^\top \mathbf{q}$  with

- (a)  $z_{\min} = -q_1, z_{\max} = \infty$  if  $\beta_2 > 0$ ;
- (b)  $z_{\min} = -\infty, z_{\max} = q_1$  if  $\beta_2 < 0$ .

6. If  $\beta_2 = 0$ , then  $r_{\min} = \beta^\top \mathbf{q}$  and  $r_{\max} = \infty$ , with

- (a)  $z_{\min} = -\infty, z_{\max} = q_2$  if  $\beta_1 > 0$ ;
- (b)  $z_{\min} = -q_2, z_{\max} = \infty$  if  $\beta_1 < 0$ .

### B.3. Integration bounds in dimension $d \geq 3$

In dimension  $d \geq 3$ , sequential sampling can also be used, but this approach is expensive relative to regular Monte Carlo. Considering that integration bounds for  $r, z_1, \dots, z_{d-1}$  are found by solving linear programs for each simulated point, this requires solving  $\mathcal{O}(Td)$  linear programs in dimension  $d$  if  $T$  Monte Carlo replications are drawn.

The forward sampling algorithm is as follows: first, obtain the lower and upper bounds for the radius,

$$r_{\min} = \max(0, \min_{\mathbf{x}} \beta^\top \mathbf{x}) \quad \text{and} \quad r_{\max} = \max(0, \max_{\mathbf{x}} \beta^\top \mathbf{x}),$$

by solving the two optimization problems subject to the inequality constraint  $\mathbf{x} \leq \mathbf{q}$ . Next, generate  $T$  univariate inverse Gaussian random variables truncated between  $r_{\min}$  and  $r_{\max}$ . Then, for each simulated value of  $r$ , proceed by forward sampling from the truncated conditional Gaussian distribution of  $z_j \mid z_1, \dots, z_{j-1}, r$ . The truncation bounds can be obtained again by solving a linear program, where

$$z_{\min,i}(r) = \min_{\mathbf{x}} (\mathbf{Q}_2\mathbf{x})_i \quad \text{and} \quad z_{\max,i}(r) = \max_{\mathbf{x}} (\mathbf{Q}_2\mathbf{x})_i$$

subject to the equality constraints  $\beta^\top \mathbf{x} = r, (\mathbf{Q}_2\mathbf{x})_j = z_j$  for all  $j \in \{1, \dots, i-1\}$  ( $i > 2$ ), and the same inequality constraint  $\mathbf{x} \leq \mathbf{q}$ . Finally, evaluate (B.2) with the simulated  $T$  draws to obtain the estimator.

## Appendix C: Proofs of the asymptotics for the MIG asymmetric kernel smoother

### C.1. Proof of Proposition 5.1

Given that the target density  $f$  is assumed to be bounded, the supremum norm  $\|f\|_\infty$  is finite. Simple calculations show that

$$\begin{aligned}\text{Var}\{\hat{f}_{n,\mathbf{H}}(\boldsymbol{\xi})\} &= n^{-1} \mathbf{E}\{k_{\beta,\boldsymbol{\xi},\mathbf{H}}(\mathbf{X})^2\} - n^{-1} [\mathbf{E}\{k_{\beta,\boldsymbol{\xi},\mathbf{H}}(\mathbf{X})\}]^2 \\ &= n^{-1} \mathbf{E}\{k_{\beta,\boldsymbol{\xi},\mathbf{H}}(\mathbf{X})^2\} - \mathcal{O}(n^{-1}\|f\|_\infty^2).\end{aligned}$$

One deduces from the multivariate normal local approximation in Theorem 3.3 that

$$\begin{aligned}\mathbf{E}\{k_{\beta,\boldsymbol{\xi},\mathbf{H}}(\mathbf{X})^2\} &= \int_{\mathcal{H}_d(\beta)} \left[ \frac{\exp\left\{-\frac{1}{2}(\mathbf{x}-\boldsymbol{\xi})^\top(\beta^\top \boldsymbol{\xi} \mathbf{H})^{-1}(\mathbf{x}-\boldsymbol{\xi})\right\}}{(2\pi)^{d/2}|\beta^\top \boldsymbol{\xi} \mathbf{H}|^{1/2}} \right]^2 f(\mathbf{x}) \, d\mathbf{x} + o_{\beta,\boldsymbol{\xi}}(1) \\ &= \frac{\{f(\boldsymbol{\xi}) + \mathcal{O}_{\beta,\boldsymbol{\xi}}(\|\mathbf{H}\|_2)\}}{(2\pi)^{d/2}|2\beta^\top \boldsymbol{\xi} \mathbf{H}|^{1/2}} \int_{\mathcal{H}_d(\beta)} \frac{\exp\left\{-\frac{1}{2}(\mathbf{x}-\boldsymbol{\xi})^\top(\frac{1}{2}\beta^\top \boldsymbol{\xi} \mathbf{H})^{-1}(\mathbf{x}-\boldsymbol{\xi})\right\}}{(2\pi)^{d/2}|\frac{1}{2}\beta^\top \boldsymbol{\xi} \mathbf{H}|^{1/2}} \, d\mathbf{x} \\ &\quad + o_{\beta,\boldsymbol{\xi}}(1) \\ &= \frac{\{f(\boldsymbol{\xi}) + \mathcal{O}_{\beta,\boldsymbol{\xi}}(\|\mathbf{H}\|_2)\}}{(4\pi\beta^\top \boldsymbol{\xi})^{d/2}|\mathbf{H}|^{1/2}} \{1 + o_{\beta,\boldsymbol{\xi}}(1)\} + o_{\beta,\boldsymbol{\xi}}(1).\end{aligned}$$

The conclusion follows.

### C.2. Proof of Proposition 5.2

For any real vectors  $\beta \in \mathbb{R}^d$ ,  $\boldsymbol{\xi} \in \mathcal{H}_d(\beta)$ , and any symmetric positive definite matrix  $\mathbf{H} \in \mathcal{S}_{++}^d$ , define the random vector

$$\mathbf{Y}_\boldsymbol{\xi} = (Y_1, \dots, Y_d) \sim \text{MIG}(\beta, \boldsymbol{\xi}, \mathbf{H}).$$

As in (3.12), note that, for all  $i, j \in \{1, \dots, d\}$ ,

$$\mathbf{E}(Y_i) = \xi_i, \quad \mathbf{E}\{(Y_i - \xi_i)(Y_j - \xi_j)\} = \text{Cov}(Y_i, Y_j) = \beta^\top \boldsymbol{\xi} \mathbf{H}_{ij}. \quad (\text{C.1})$$

By a second order stochastic mean value theorem (Aliprantis and Border, 2006, Theorem 18.18), one has

$$\begin{aligned}f(\mathbf{Y}_\boldsymbol{\xi}) - f(\boldsymbol{\xi}) &= \sum_{i=1}^d (Y_i - \xi_i) \frac{\partial}{\partial \xi_i} f(\boldsymbol{\xi}) + \frac{1}{2} \sum_{i,j=1}^d (Y_i - \xi_i)(Y_j - \xi_j) \frac{\partial^2}{\partial \xi_i \partial \xi_j} f(\boldsymbol{\xi}) \\ &\quad + \frac{1}{2} \sum_{i,j=1}^d (Y_i - \xi_i)(Y_j - \xi_j) \left\{ \frac{\partial^2}{\partial \xi_i \partial \xi_j} f(\boldsymbol{\zeta}_\boldsymbol{\xi}) - \frac{\partial^2}{\partial \xi_i \partial \xi_j} f(\boldsymbol{\xi}) \right\},\end{aligned} \quad (\text{C.2})$$

for some random vector  $\zeta_{\boldsymbol{\xi}} \in \mathcal{H}_d(\boldsymbol{\beta})$  on the line segment joining  $\mathbf{Y}_{\boldsymbol{\xi}}$  and  $\boldsymbol{\xi}$ . Given that it was assumed that the second order partial derivatives of  $f$  are uniformly continuous on the half-space  $\mathcal{H}_d(\boldsymbol{\beta})$ , then for any given  $\varepsilon \in (0, \infty)$ , there exists a real number  $\delta_{d,\boldsymbol{\beta},\varepsilon} \in (0, 1]$  such that, uniformly for  $\boldsymbol{\xi}, \boldsymbol{\xi}' \in \mathcal{H}_d(\boldsymbol{\beta})$ ,

$$\|\boldsymbol{\xi}' - \boldsymbol{\xi}\|_1 \leq \delta_{d,\boldsymbol{\beta},\varepsilon} \Rightarrow \left| \frac{\partial^2}{\partial \xi_i \partial \xi_j} f(\boldsymbol{\xi}') - \frac{\partial^2}{\partial \xi_i \partial \xi_j} f(\boldsymbol{\xi}) \right| < \varepsilon.$$

Therefore, by fixing  $\varepsilon \in (0, \infty)$ , taking the expectation on both sides of (C.2), and then using (C.1), one can bound the bias as follows:

$$\begin{aligned} & \left| \text{Bias}\{\hat{f}_{n,\mathbf{H}}(\boldsymbol{\xi})\} - \frac{1}{2} \boldsymbol{\beta}^\top \boldsymbol{\xi} \sum_{i,j=1}^d \mathbf{H}_{ij} \frac{\partial^2}{\partial \xi_i \partial \xi_j} f(\boldsymbol{\xi}) \right| \\ &= \left| \frac{1}{2} \sum_{i,j=1}^d \mathbb{E}\{(Y_i - \xi_i)(Y_j - \xi_j)\} \left\{ \frac{\partial^2}{\partial \xi_i \partial \xi_j} f(\zeta_{\boldsymbol{\xi}}) - \frac{\partial^2}{\partial \xi_i \partial \xi_j} f(\boldsymbol{\xi}) \right\} \right| \\ &\leq \frac{1}{2} \sum_{i,j=1}^d \mathbb{E} \left[ |Y_i - \xi_i| |Y_j - \xi_j| \left| \frac{\partial^2}{\partial \xi_i \partial \xi_j} f(\zeta_{\boldsymbol{\xi}}) - \frac{\partial^2}{\partial \xi_i \partial \xi_j} f(\boldsymbol{\xi}) \right| \mathbf{1}_{\{\|\mathbf{Y}_{\boldsymbol{\xi}} - \boldsymbol{\xi}\|_1 \leq \delta_{d,\boldsymbol{\beta},\varepsilon}\}} \right] \\ &\quad + \frac{1}{2} \sum_{i,j=1}^d \mathbb{E} \left[ |Y_i - \xi_i| |Y_j - \xi_j| \left| \frac{\partial^2}{\partial \xi_i \partial \xi_j} f(\zeta_{\boldsymbol{\xi}}) - \frac{\partial^2}{\partial \xi_i \partial \xi_j} f(\boldsymbol{\xi}) \right| \mathbf{1}_{\{\|\mathbf{Y}_{\boldsymbol{\xi}} - \boldsymbol{\xi}\|_1 > \delta_{d,\boldsymbol{\beta},\varepsilon}\}} \right] \\ &\equiv \Delta_1 + \Delta_2. \end{aligned} \tag{C.3}$$

If one applies the uniform continuity of the second order partial derivatives together with the fact that  $\|\zeta_{\boldsymbol{\xi}} - \boldsymbol{\xi}\|_1 \leq \|\mathbf{Y}_{\boldsymbol{\xi}} - \boldsymbol{\xi}\|_1$ , followed by the Cauchy-Schwarz inequality, then (C.1), and then Jensen's inequality, one gets

$$\begin{aligned} \Delta_1 &\leq \frac{\varepsilon}{2} \sum_{i,j=1}^d \sqrt{\mathbb{E}(|Y_i - \xi_i|^2)} \sqrt{\mathbb{E}(|Y_j - \xi_j|^2)} = \frac{\varepsilon}{2} \boldsymbol{\beta}^\top \boldsymbol{\xi} \left\{ \sum_{i=1}^d \sqrt{\mathbf{H}_{ii}} \right\}^2 \\ &\leq \frac{\varepsilon}{2} \boldsymbol{\beta}^\top \boldsymbol{\xi} \left\{ d \sum_{i=1}^d \mathbf{H}_{ii} \right\} \leq \frac{\varepsilon d^2}{2} \boldsymbol{\beta}^\top \boldsymbol{\xi} \|\mathbf{H}\|_2. \end{aligned}$$

Next, the second order partial derivatives were also assumed to be bounded, say by  $M_d \in (0, \infty)$ . Therefore, applying the bound  $M_d$  on the two second order partial derivatives in  $\Delta_2$ , followed by a moment version of Chernoff's inequality, and then using the elementary inequality  $x \leq \exp(x)$ , one finds

$$\begin{aligned} \Delta_2 &\leq \frac{2M_d}{2} \mathbb{E} (\|\mathbf{Y}_{\boldsymbol{\xi}} - \boldsymbol{\xi}\|_1^2 \mathbf{1}_{\{\|\mathbf{Y}_{\boldsymbol{\xi}} - \boldsymbol{\xi}\|_1 > \delta_{d,\boldsymbol{\beta},\varepsilon}\}}) \\ &\leq M_d \inf_{s \in (0, \infty)} \exp(-s\delta_{d,\boldsymbol{\beta},\varepsilon}) \mathbb{E} \{ \|\mathbf{Y}_{\boldsymbol{\xi}} - \boldsymbol{\xi}\|_1^2 \exp(s\|\mathbf{Y}_{\boldsymbol{\xi}} - \boldsymbol{\xi}\|_1) \} \\ &\leq M_d \inf_{s \in (0, \infty)} \exp(-s\delta_{d,\boldsymbol{\beta},\varepsilon}) \mathbb{E} [\exp\{(2+s)\|\mathbf{Y}_{\boldsymbol{\xi}} - \boldsymbol{\xi}\|_1\}] \\ &\leq e^2 M_d \inf_{t \in (2, \infty)} \exp(-t\delta_{d,\boldsymbol{\beta},\varepsilon}) \mathbb{E} [\exp\{t\|\mathbf{Y}_{\boldsymbol{\xi}} - \boldsymbol{\xi}\|_1\}]. \end{aligned}$$

Let  $\mathbf{Z} \sim \mathcal{N}_d(\mathbf{0}_d, \boldsymbol{\beta}^\top \boldsymbol{\xi} \mathbf{H})$ . By the asymptotic normality in (3.13) and the continuous mapping theorem, one obtains

$$\Delta_2 = \mathcal{O} \left[ \inf_{t \in (2, \infty)} \exp(-t\delta_{d, \boldsymbol{\beta}, \varepsilon}) \mathbb{E} \{ \exp(t\|\mathbf{Z}\|_1) \} \right].$$

By optimizing this Chernoff bound, one has, say,  $\Delta_2 = \mathcal{O}(\|\mathbf{H}\|_2^{100})$  provided that the sequences  $\varepsilon = \varepsilon(\mathbf{H}) \in (0, \infty)$  and  $\delta_{d, \boldsymbol{\beta}, \varepsilon} = \delta_{d, \boldsymbol{\beta}, \varepsilon}(\mathbf{H}) \in (0, 1]$  are chosen to converge slowly enough to 0 as  $\|\mathbf{H}\|_2 \rightarrow 0$ .

It follows that  $\Delta_1 + \Delta_2$  in (C.3) is  $o(\boldsymbol{\beta}^\top \boldsymbol{\xi} \|\mathbf{H}\|_2)$ . This concludes the proof.

### C.3. Proof of Theorem 5.5

First note that

$$\hat{f}_{n, \mathbf{H}}(\boldsymbol{\xi}) - \mathbb{E} \{ \hat{f}_{n, \mathbf{H}}(\boldsymbol{\xi}) \} = \frac{1}{n} \sum_{i=1}^n Z_{i, \mathbf{H}}(\boldsymbol{\xi}),$$

where

$$Z_{i, \mathbf{H}}(\boldsymbol{\xi}) = k_{\boldsymbol{\beta}, \boldsymbol{\xi}, \mathbf{H}}(\mathbf{X}_i) - \mathbb{E} \{ k_{\boldsymbol{\beta}, \boldsymbol{\xi}, \mathbf{H}}(\mathbf{X}_i) \}.$$

Like the observations  $\mathbf{X}_1, \dots, \mathbf{X}_n$ , the random variables  $Z_{1, \mathbf{H}}(\boldsymbol{\xi}), \dots, Z_{n, \mathbf{H}}(\boldsymbol{\xi})$  are independent and identically distributed.

Calling on the material in, e.g., Section 1.9.3 of [Serfling \(1980\)](#), the asymptotic normality of  $n^{1/2}|\mathbf{H}|^{1/4}[\hat{f}_{n, \mathbf{H}}(\boldsymbol{\xi}) - \mathbb{E}\{\hat{f}_{n, \mathbf{H}}(\boldsymbol{\xi})\}]$  will be proved if one verifies the following Lindeberg condition for double arrays: for every real  $\varepsilon \in (0, \infty)$ ,

$$\lim_{n \rightarrow \infty} \frac{1}{s_{\mathbf{H}}^2} \mathbb{E} \{ |Z_{1, \mathbf{H}}(\boldsymbol{\xi})|^2 \mathbf{1}_{(\varepsilon n^{1/2} s_{\mathbf{H}}, +\infty)}(|Z_{1, \mathbf{H}}(\boldsymbol{\xi})|) \} = 0, \quad (\text{C.4})$$

where  $s_{\mathbf{H}}^2 = \mathbb{E}\{|Z_{1, \mathbf{H}}(\boldsymbol{\xi})|^2\}$  and  $\mathbf{H} = \mathbf{H}(n)$  is such that  $\|\mathbf{H}\|_2 \rightarrow 0$ .

The condition (C.4) is verified below. From the uniform bound on  $k_{\boldsymbol{\beta}, \boldsymbol{\xi}, \mathbf{H}}(\cdot)$  in Lemma D.1, it is known that

$$|Z_{1, \mathbf{H}}(\boldsymbol{\xi})| = \mathcal{O}_{\boldsymbol{\beta}, \boldsymbol{\xi}}(|\mathbf{H}|^{-1/2}).$$

Furthermore, by the asymptotics of the pointwise variance in Proposition 5.1 under the assumption that  $f$  is Lipschitz continuous and bounded on the half-space  $\mathcal{H}_d(\boldsymbol{\beta})$ , one has

$$s_{\mathbf{H}} = |\mathbf{H}|^{-1/4} \sqrt{\frac{f(\boldsymbol{\xi})}{(4\pi \boldsymbol{\beta}^\top \boldsymbol{\xi})^{d/2}}} \{1 + o_{\boldsymbol{\beta}, \boldsymbol{\xi}}(1)\}.$$

Therefore, by combining the last two equations, one gets

$$\frac{|Z_{1, \mathbf{H}}(\boldsymbol{\xi})|}{n^{1/2} s_{\mathbf{H}}} = \mathcal{O}_{\boldsymbol{\beta}, \boldsymbol{\xi}}(n^{-1/2} |\mathbf{H}|^{-1/4}) \longrightarrow 0 \quad (\text{C.5})$$

whenever  $n^{1/2}|\mathbf{H}|^{1/4} \rightarrow \infty$  as  $n \rightarrow \infty$ . The convergence to zero in (C.5) shows that (C.4) holds because  $\varepsilon \in (0, \infty)$  being fixed implies that the indicator function in (C.4) is equal to zero for  $n$  large enough, independently of  $\omega$ .

Hence, by Proposition 5.1 again, one deduces that

$$\begin{aligned} & n^{1/2}|\mathbf{H}|^{1/4} \left[ \hat{f}_{n,\mathbf{H}}(\boldsymbol{\xi}) - \mathbb{E}\{\hat{f}_{n,\mathbf{H}}(\boldsymbol{\xi})\} \right] \\ &= n^{1/2}|\mathbf{H}|^{1/4} \frac{1}{n} \sum_{i=1}^n Z_{i,\mathbf{H}}(\boldsymbol{\xi}) \rightsquigarrow \mathcal{N}_d \left[ 0, \frac{f(\boldsymbol{\xi})}{(4\pi\boldsymbol{\beta}^\top \boldsymbol{\xi})^{d/2}} \right]. \end{aligned}$$

This concludes the proof.

## Appendix D: Technical lemmas

For ease of reading, the definition of the MIG density from (3.11) is recalled below. For every  $\mathbf{x} \in \mathcal{H}_d(\boldsymbol{\beta})$ , one has

$$\begin{aligned} k_{\boldsymbol{\beta},\boldsymbol{\xi},\boldsymbol{\Omega}}(\mathbf{x}) &= (2\pi)^{-d/2} \boldsymbol{\beta}^\top \boldsymbol{\xi} |\boldsymbol{\Omega}|^{-1/2} (\boldsymbol{\beta}^\top \mathbf{x})^{-(d/2+1)} \\ &\quad \times \exp \left\{ -\frac{1}{2\boldsymbol{\beta}^\top \mathbf{x}} (\mathbf{x} - \boldsymbol{\xi})^\top \boldsymbol{\Omega}^{-1} (\mathbf{x} - \boldsymbol{\xi}) \right\}. \end{aligned} \quad (\text{D.1})$$

### D.1. Uniform bound on the MIG density

A uniform upper bound on the MIG density (D.1) is stated and proved below.

**Lemma D.1.** *For any real vectors  $\boldsymbol{\beta} \in \mathbb{R}^d$  and  $\boldsymbol{\xi} \in \mathcal{H}_d(\boldsymbol{\beta})$ , and any symmetric positive definite matrix  $\boldsymbol{\Omega}$ , one has*

$$\begin{aligned} \sup_{\mathbf{x} \in \mathcal{H}_d(\boldsymbol{\beta})} k_{\boldsymbol{\beta},\boldsymbol{\xi},\boldsymbol{\Omega}}(\mathbf{x}) &\leq (2\pi)^{-d/2} \boldsymbol{\beta}^\top \boldsymbol{\xi} |\boldsymbol{\Omega}|^{-1/2} \\ &\quad \times \max \left\{ \frac{2}{\boldsymbol{\beta}^\top \boldsymbol{\xi}}, \frac{(d/2+1) 8 \|\boldsymbol{\Omega}\|_2 \|\boldsymbol{\beta}\|_2^2}{e (\boldsymbol{\beta}^\top \boldsymbol{\xi})^2} \right\}^{d/2+1}, \end{aligned}$$

where  $\|\boldsymbol{\Omega}\|_2$  denotes the spectral norm of  $\boldsymbol{\Omega}$ . In particular, if one assumes that  $\|\boldsymbol{\Omega}\|_2 \rightarrow 0$ , then one has

$$\sup_{\mathbf{x} \in \mathcal{H}_d(\boldsymbol{\beta})} k_{\boldsymbol{\beta},\boldsymbol{\xi},\boldsymbol{\Omega}}(\mathbf{x}) = \mathcal{O}_{\boldsymbol{\beta},\boldsymbol{\xi}}(|\boldsymbol{\Omega}|^{-1/2}).$$

*Proof of Lemma D.1.* There are two cases to consider, namely

$$(i) \quad \|\mathbf{x} - \boldsymbol{\xi}\|_2 < \frac{\boldsymbol{\beta}^\top \boldsymbol{\xi}}{2\|\boldsymbol{\beta}\|_2}, \quad (ii) \quad \|\mathbf{x} - \boldsymbol{\xi}\|_2 \geq \frac{\boldsymbol{\beta}^\top \boldsymbol{\xi}}{2\|\boldsymbol{\beta}\|_2}.$$

In the first case, an application of the Cauchy–Schwarz inequality yields

$$|\boldsymbol{\beta}^\top \mathbf{x} - \boldsymbol{\beta}^\top \boldsymbol{\xi}| = |\boldsymbol{\beta}^\top (\mathbf{x} - \boldsymbol{\xi})| \leq \|\boldsymbol{\beta}\|_2 \|\mathbf{x} - \boldsymbol{\xi}\|_2 < \frac{\boldsymbol{\beta}^\top \boldsymbol{\xi}}{2}.$$

From this, one deduces that  $\beta^\top \mathbf{x} \geq \beta^\top \boldsymbol{\xi}/2$ , or equivalently  $(\beta^\top \mathbf{x})^{-1} \leq 2/(\beta^\top \boldsymbol{\xi})$ . Therefore, if the exponential is bounded above by 1 in  $k_{\beta, \boldsymbol{\xi}, \boldsymbol{\Omega}}(\mathbf{x})$ , one gets

$$k_{\beta, \boldsymbol{\xi}, \boldsymbol{\Omega}}(\mathbf{x}) \leq (2\pi)^{-d/2} \beta^\top \boldsymbol{\xi} |\boldsymbol{\Omega}|^{-1/2} \left( \frac{2}{\beta^\top \boldsymbol{\xi}} \right)^{d/2+1}. \quad (\text{D.2})$$

In the second case, one initially observes that the eigenvalues of  $\boldsymbol{\Omega}^{-1}$  are the inverses of the eigenvalues of  $\boldsymbol{\Omega}$ . Given that  $\|\boldsymbol{\Omega}\|_2$  corresponds to the largest eigenvalue of  $\boldsymbol{\Omega}$ ,  $\|\boldsymbol{\Omega}\|_2^{-1}$  corresponds to the smallest eigenvalue of  $\boldsymbol{\Omega}^{-1}$ . One deduces the lower bound

$$(\mathbf{x} - \boldsymbol{\xi})^\top \boldsymbol{\Omega}^{-1} (\mathbf{x} - \boldsymbol{\xi}) \geq \|\boldsymbol{\Omega}\|_2^{-1} \|\mathbf{x} - \boldsymbol{\xi}\|_2^2 \geq \|\boldsymbol{\Omega}\|_2^{-1} \frac{(\beta^\top \boldsymbol{\xi})^2}{4\|\boldsymbol{\beta}\|_2^2}.$$

Hence, with the notation  $y = (\beta^\top \mathbf{x})^{-1}$ , one has

$$\begin{aligned} k_{\beta, \boldsymbol{\xi}, \boldsymbol{\Omega}}(\mathbf{x}) &= (2\pi)^{-d/2} \beta^\top \boldsymbol{\xi} |\boldsymbol{\Omega}|^{-1/2} y^{d/2+1} \exp \left\{ -\frac{y}{2} (\mathbf{x} - \boldsymbol{\xi})^\top \boldsymbol{\Omega}^{-1} (\mathbf{x} - \boldsymbol{\xi}) \right\} \\ &\leq (2\pi)^{-d/2} \beta^\top \boldsymbol{\xi} |\boldsymbol{\Omega}|^{-1/2} y^{d/2+1} \exp \left\{ -y \frac{(\beta^\top \boldsymbol{\xi})^2}{8\|\boldsymbol{\Omega}\|_2 \|\boldsymbol{\beta}\|_2^2} \right\}. \end{aligned}$$

For any positive constant  $c \in (0, \infty)$ , straightforward calculations show that the function  $y \mapsto y^{d/2+1} \exp(-y/c)$  is maximized at the point  $y = (d/2 + 1)c$ . Therefore, one finds

$$k_{\beta, \boldsymbol{\xi}, \boldsymbol{\Omega}}(\mathbf{x}) \leq (2\pi)^{-d/2} \beta^\top \boldsymbol{\xi} |\boldsymbol{\Omega}|^{-1/2} \left\{ \frac{(d/2 + 1) 8\|\boldsymbol{\Omega}\|_2 \|\boldsymbol{\beta}\|_2^2}{e (\beta^\top \boldsymbol{\xi})^2} \right\}^{d/2+1}. \quad (\text{D.3})$$

The conclusion then follows from (D.2) and (D.3).  $\square$

## D.2. Maximum likelihood estimator (MLE)

The form of the MLE for the parameters  $\boldsymbol{\xi}$  and  $\boldsymbol{\Omega}$  of the MIG density (D.1) is stated and derived below under the assumption that the parameter  $\boldsymbol{\beta}$  is known.

**Lemma D.2.** *Let the real vector  $\boldsymbol{\beta} \in \mathbb{R}^d$  be given. The MLE for the pair  $(\boldsymbol{\xi}, \boldsymbol{\Omega})$  of the MIG( $\boldsymbol{\beta}, \boldsymbol{\xi}, \boldsymbol{\Omega}$ ) distribution is given by  $(\boldsymbol{\xi}_n^*, \boldsymbol{\Omega}_n^*)$ , where*

$$\boldsymbol{\xi}_n^* = \frac{1}{n} \sum_{i=1}^n \mathbf{x}_i \equiv \bar{\mathbf{x}}_n, \quad \boldsymbol{\Omega}_n^* = \frac{1}{n} \sum_{i=1}^n \frac{1}{\beta^\top \mathbf{x}_i} (\mathbf{x}_i - \bar{\mathbf{x}}_n)(\mathbf{x}_i - \bar{\mathbf{x}}_n)^\top.$$

*Proof of Lemma D.2.* The log-likelihood of the MIG( $\boldsymbol{\beta}, \boldsymbol{\xi}, \boldsymbol{\Omega}$ ) distribution is

$$\begin{aligned} \ell(\boldsymbol{\xi}, \boldsymbol{\Omega}) &= \sum_{i=1}^n \ln \{k_{\beta, \boldsymbol{\xi}, \boldsymbol{\Omega}}(\mathbf{x}_i)\} \\ &= -\frac{nd}{2} \ln(2\pi) + n \ln(\beta^\top \boldsymbol{\xi}) + \frac{n}{2} \ln |\boldsymbol{\Omega}^{-1}| - (d/2 + 1) \sum_{i=1}^n \ln(\beta^\top \mathbf{x}_i) \\ &\quad - \frac{1}{2} \sum_{i=1}^n \frac{1}{\beta^\top \mathbf{x}_i} (\mathbf{x}_i - \boldsymbol{\xi})^\top \boldsymbol{\Omega}^{-1} (\mathbf{x}_i - \boldsymbol{\xi}). \end{aligned}$$

First, consider the derivative with respect to  $\Omega^{-1}$ . Given that

$$\frac{\partial}{\partial \Omega^{-1}} |\Omega^{-1}| = |\Omega^{-1}| (\Omega^{-1})^{-1} = |\Omega^{-1}| \Omega$$

and

$$\frac{\partial}{\partial \Omega^{-1}} (\mathbf{x}_i - \boldsymbol{\xi})^\top \Omega^{-1} (\mathbf{x}_i - \boldsymbol{\xi}) = (\mathbf{x}_i - \boldsymbol{\xi})(\mathbf{x}_i - \boldsymbol{\xi})^\top,$$

one has

$$\begin{aligned} \frac{\partial}{\partial \Omega^{-1}} \ell(\boldsymbol{\xi}, \Omega) &= \frac{n}{2} \Omega - \frac{1}{2} \sum_{i=1}^n \frac{1}{\boldsymbol{\beta}^\top \mathbf{x}_i} (\mathbf{x}_i - \boldsymbol{\xi})(\mathbf{x}_i - \boldsymbol{\xi})^\top = \mathbf{0}_{d \times d} \\ &\Leftrightarrow \Omega = \frac{1}{n} \sum_{i=1}^n \frac{1}{\boldsymbol{\beta}^\top \mathbf{x}_i} (\mathbf{x}_i - \boldsymbol{\xi})(\mathbf{x}_i - \boldsymbol{\xi})^\top. \end{aligned}$$

Alternatively, one can write the expression for  $\Omega$  as follows:

$$\Omega = \frac{1}{n} \sum_{i=1}^n \frac{\mathbf{x}_i \mathbf{x}_i^\top}{\boldsymbol{\beta}^\top \mathbf{x}_i} - \frac{1}{n} \sum_{i=1}^n \frac{\mathbf{x}_i \boldsymbol{\xi}^\top}{\boldsymbol{\beta}^\top \mathbf{x}_i} - \frac{1}{n} \sum_{i=1}^n \frac{\boldsymbol{\xi} \mathbf{x}_i^\top}{\boldsymbol{\beta}^\top \mathbf{x}_i} + \frac{1}{n} \sum_{i=1}^n \frac{\boldsymbol{\xi} \boldsymbol{\xi}^\top}{\boldsymbol{\beta}^\top \mathbf{x}_i}.$$

Consider now the derivative with respect to  $\boldsymbol{\xi}$ . Given that

$$\frac{\partial}{\partial \boldsymbol{\xi}} \boldsymbol{\beta}^\top \boldsymbol{\xi} = \boldsymbol{\beta}$$

and

$$\frac{\partial}{\partial \boldsymbol{\xi}} (\mathbf{x}_i - \boldsymbol{\xi})^\top \Omega^{-1} (\mathbf{x}_i - \boldsymbol{\xi}) = -2\Omega^{-1} (\mathbf{x}_i - \boldsymbol{\xi}),$$

one has

$$\begin{aligned} \frac{\partial}{\partial \boldsymbol{\xi}} \ell(\boldsymbol{\xi}, \Omega) &= \mathbf{0}_d \\ &\Leftrightarrow \frac{n\boldsymbol{\beta}}{\boldsymbol{\beta}^\top \boldsymbol{\xi}} + \Omega^{-1} \sum_{i=1}^n \frac{1}{\boldsymbol{\beta}^\top \mathbf{x}_i} (\mathbf{x}_i - \boldsymbol{\xi}) = \mathbf{0}_d \\ &\Leftrightarrow \frac{n\Omega\boldsymbol{\beta}}{\boldsymbol{\beta}^\top \boldsymbol{\xi}} + \sum_{i=1}^n \frac{1}{\boldsymbol{\beta}^\top \mathbf{x}_i} (\mathbf{x}_i - \boldsymbol{\xi}) = \mathbf{0}_d \\ &\Leftrightarrow \sum_{i=1}^n \frac{\mathbf{x}_i}{\boldsymbol{\beta}^\top \boldsymbol{\xi}} - \sum_{i=1}^n \frac{\mathbf{x}_i}{\boldsymbol{\beta}^\top \mathbf{x}_i} - \sum_{i=1}^n \frac{\boldsymbol{\xi}}{\boldsymbol{\beta}^\top \boldsymbol{\xi}} + \sum_{i=1}^n \frac{\boldsymbol{\xi}}{\boldsymbol{\beta}^\top \mathbf{x}_i} + \sum_{i=1}^n \frac{\mathbf{x}_i}{\boldsymbol{\beta}^\top \mathbf{x}_i} - \sum_{i=1}^n \frac{\boldsymbol{\xi}}{\boldsymbol{\beta}^\top \mathbf{x}_i} = \mathbf{0}_d \\ &\Leftrightarrow \frac{1}{\boldsymbol{\beta}^\top \boldsymbol{\xi}} \sum_{i=1}^n \mathbf{x}_i - \frac{n\boldsymbol{\xi}}{\boldsymbol{\beta}^\top \boldsymbol{\xi}} = \mathbf{0}_d \\ &\Leftrightarrow \boldsymbol{\xi} = \frac{1}{n} \sum_{i=1}^n \mathbf{x}_i. \end{aligned}$$

The conclusion follows.  $\square$



### D.3. Hessian of the MIG density

In this section, the Hessian of the MIG density (D.1) is calculated.

As shown in Corollary 5.4, the bandwidth matrix parameter that minimizes the asymptotic MISE of the MIG asymmetric kernel smoother defined in (5.1) is a function of the Hessian of the target density. When using the MIG as a plug-in, an explicit expression is needed because numerical differentiation can yield infinite entries for the Hessian matrix.

The gradient of the MIG( $\beta, \xi, \Omega$ ) log-density with respect to the data is

$$\frac{\partial}{\partial \mathbf{x}} \ln\{f(\mathbf{x})\} = -\frac{(1 + d/2)\beta + \Omega^{-1}(\mathbf{x} - \xi)}{\beta^\top \mathbf{x}} + \frac{(\mathbf{x} - \xi)^\top \Omega^{-1}(\mathbf{x} - \xi)\beta}{2(\beta^\top \mathbf{x})^2},$$

while the Hessian is

$$\begin{aligned} \frac{\partial}{\partial \mathbf{x} \partial \mathbf{x}^\top} \ln\{f(\mathbf{x})\} &= -\frac{\Omega^{-1}}{\beta^\top \mathbf{x}} + \frac{(1 + d/2)\beta\beta^\top + \Omega^{-1}(\mathbf{x} - \xi)\beta^\top + \beta(\mathbf{x} - \xi)^\top \Omega^{-1}}{(\beta^\top \mathbf{x})^2} \\ &\quad - \frac{(\mathbf{x} - \xi)^\top \Omega^{-1}(\mathbf{x} - \xi)\beta\beta^\top}{(\beta^\top \mathbf{x})^3}. \end{aligned}$$

The Hessian of the density is then easily derived as

$$\begin{aligned} \frac{\partial^2}{\partial \mathbf{x} \partial \mathbf{x}^\top} f(\mathbf{x}) &= \frac{\partial^2}{\partial \mathbf{x} \partial \mathbf{x}^\top} \exp[\ln\{f(\mathbf{x})\}] \\ &= \frac{\partial}{\partial \mathbf{x}} \left( \exp[\ln\{f(\mathbf{x})\}] \frac{\partial}{\partial \mathbf{x}^\top} \ln\{f(\mathbf{x})\} \right) \\ &= f(\mathbf{x}) \left[ \frac{\partial}{\partial \mathbf{x}} \ln\{f(\mathbf{x})\} \frac{\partial}{\partial \mathbf{x}^\top} \ln\{f(\mathbf{x})\} + \frac{\partial^2}{\partial \mathbf{x} \partial \mathbf{x}^\top} \ln\{f(\mathbf{x})\} \right]. \end{aligned}$$

### Appendix E: Reproducibility

The R codes that generated the figures, the simulation study results and the real-data application can be found [here](#). The R package `mig` implements the kernel density estimator and is available from the CRAN and Github at <https://github.com/lbelzile/mig>.

### Appendix F: List of abbreviations

IG	inverse Gaussian
iid	independent and identically distributed
LCV	likelihood cross-validation
MIG	multivariate inverse Gaussian
MISE	mean integrated squared error
RMISE	root mean integrated squared error

## Funding

Belzile acknowledges funding from the Natural Sciences and Engineering Research Council of Canada through grant number RGPIN-2022-05001. Genest's research and Ouimet's current postdoctoral fellowship are funded through the Canada Research Chairs Program (Grant 950-231937) and the Natural Sciences and Engineering Research Council of Canada (Grant RGPIN-2024-04088 to C. Genest). Ouimet also wishes to acknowledge past support from a CRM-Simons postdoctoral fellowship from the Centre de recherches mathématiques (Montréal, Canada) and the Simons Foundation.

## References

- AL-HUSSAINI, E. K. and ABD-EL-HAKIM, N. S. (1981). Bivariate inverse Gaussian distribution. *Ann. Inst. Statist. Math.* **33** 57–66. <https://doi.org/10.1007/bf02480919> MR613202
- ALIPRANTIS, C. D. and BORDER, K. C. (2006). *Infinite Dimensional Analysis*, third ed. Springer Berlin, Heidelberg. <https://doi.org/10.1007/3-540-29587-9> MR2378491
- AZZALINI, A. and CAPITANIO, A. (1999). Statistical applications of the multivariate skew normal distribution. *J. R. Stat. Soc. Ser. B Stat. Methodol.* **61** 579–602. <https://doi.org/10.1111/1467-9868.00194> MR1707862
- BALAKRISHNAN, N. and LAI, C. D. (2009). *Continuous Bivariate Distributions*, Second ed. Springer, Dordrecht. <https://doi.org/10.1007/b101765> MR2840643
- BARNDORFF-NIELSEN, O. and BLÆSILD, P. (1983). Reproductive exponential families. *Ann. Statist.* **11** 770–782. <https://doi.org/10.1214/aos/1176346244> MR707928
- BARNDORFF-NIELSEN, O. E., BLÆSILD, P. and SESHADRI, V. (1992). Multivariate distributions with generalized inverse Gaussian marginals, and associated Poisson mixtures. *Canad. J. Statist.* **20** 109–120. <https://doi.org/10.2307/3315462> MR1183075
- BOUEZMARNI, T. and SCAILLET, O. (2005). Consistency of asymmetric kernel density estimators and smoothed histograms with application to income data. *Econom. Theor.* **21** 390–412. <https://doi.org/10.1017/s0266466605050218> MR2179543
- BOWMAN, A. W. (1984). An alternative method of cross-validation for the smoothing of density estimates. *Biometrika* **71** 353–360. <https://doi.org/10.1093/biomet/71.2.353> MR767163
- CARTER, A. V. (2002). Deficiency distance between multinomial and multivariate normal experiments. *Ann. Statist.* **30** 708–730. <https://doi.org/10.1214/aos/2f1028674839> MR1922539
- CHACÓN, J. E. and DUONG, T. (2018). *Multivariate Kernel Smoothing and Its Applications*. CRC Press, Boca Raton, FL. <https://doi.org/10.1201/9780429485572> MR3822372

- COEURJOLLY, J. F. and TRÉPANIÉ, J. R. (2020). The median of a jittered Poisson distribution. *Metrika* **83** 837–851. [MR4135709](#)
- CRESSIE, N. (1978). A finely tuned continuity correction. *Ann. Inst. Statist. Math.* **30** 435–442. <https://doi.org/10.1007/bf02480234> [MR538319](#)
- DUONG, T. and HAZELTON, M. L. (2003). Plug-in bandwidth matrices for bivariate kernel density estimation. *J. Nonparametr. Stat.* **15** 17–30. <https://doi.org/10.1080/10485250306039> [MR1958957](#)
- ESSEEN, C. G. (1945). Fourier analysis of distribution functions. A mathematical study of the Laplace-Gaussian law. *Acta Math.* **77** 1–125. <https://doi.org/10.1007/bf02392223> [MR14626](#)
- FELLER, W. (1971). *An Introduction to Probability Theory and Its Applications. Vol. II*, Second ed. John Wiley & Sons, Inc., New York, NY. [MR0270403](#)
- GENEST, C. and NEŠLEHOVÁ, J. (2012). Copulas and copula models. In *Encyclopedia of Environmetrics*, (A. H. El-Shaarawi and W. W. Piegorsch, eds.) **2** 541–553. Wiley, Chichester. <https://doi.org/10.1002/9780470057339.vnn079>
- GENZ, A. and BRETZ, F. (2009). *Computation of Multivariate Normal and t Probabilities*. Springer Berlin, Heidelberg. <https://doi.org/10.1007/978-3-642-01689-9> [MR2840595](#)
- GIBBS, A. L. and SU, F. E. (2002). On choosing and bounding probability metrics. *Int. Stat. Rev.* **70** 419–435. <https://doi.org/10.2307/1403865>
- GINER, G. and SMYTH, G. K. (2016). `statmod`: Probability Calculations for the Inverse Gaussian Distribution. *The R Journal* **8** 339–351. <https://doi.org/10.32614/rj-2016-024>
- GOVINDARAJULU, Z. (1965). Normal approximations to the classical discrete distributions. *Sankhyā Ser. A* **27** 143–172. [MR207011](#)
- HABBEMA, J., HERMANS, J. and VAN DEN BROEK, K. (1974). A step-wise discrimination analysis program using density estimation. In *Compstat 1974: Proceedings in Computational Statistics* (G. BRUCKMAN, ed.) 101–110. Physica-Verlag, Vienna.
- HINTZ, E., HOFERT, M. and LEMIEUX, C. (2021). Normal variance mixtures: distribution, density and parameter estimation. *Comput. Statist. Data Anal.* **157** Paper No. 107175, 25 pp. <https://doi.org/10.1016/j.csda.2021.107175> [MR4204413](#)
- HIRUKAWA, M. (2018). *Asymmetric Kernel Smoothing*. Springer, Singapore. <https://doi.org/10.1007/978-981-10-5466-2> [MR3821525](#)
- IYENGAR, S. (1985). Hitting lines with two-dimensional Brownian motion. *SIAM J. Appl. Math.* **45** 983–989. <https://doi.org/10.1137/0145060> [MR813460](#)
- JOE, H., SESHADRI, V. and ARNOLD, B. C. (2012). Multivariate inverse Gaussian and skew-normal densities. *Statist. Probab. Lett.* **82** 2244–2251. <https://doi.org/10.1016/j.spl.2012.08.004> [MR2979762](#)
- JOHNSON, N. L., KOTZ, S. and BALAKRISHNAN, N. (1994). *Continuous Univariate Distributions. Vol. 1*, Second ed. John Wiley & Sons, Inc., New York, NY. [MR1299979](#)
- JONES, M. C. (1993). Simple boundary correction for kernel density estimation.

- Stat. Comput.* **3** 135–146. <https://doi.org/10.1007/bf00147776>
- KOCHERLAKOTA, S. (1986). The bivariate inverse Gaussian distribution: an introduction. *Comm. Statist. A—Theory Methods* **15** 1081–1112. <https://doi.org/10.1080/03610928608829171> MR836585
- KOKONENDJI, C. C. and SOMÉ, S. M. (2018). On multivariate associated kernels to estimate general density functions. *J. Korean Statist. Soc.* **47** 112–126. <https://doi.org/10.1016/j.jkss.2017.10.002> MR3760293
- KOKONENDJI, C. C. and SOMÉ, S. M. (2021). Bayesian bandwidths in semi-parametric modelling for nonnegative orthant data with diagnostics. *Stats* **4** 162–183. <https://doi.org/10.3390/stats4010013>
- KOLASSA, J. E. (1994). *Series Approximation Methods in Statistics*. Springer-Verlag, New York, NY. <https://doi.org/10.1007/978-1-4757-4275-6> MR1295242
- KUMAR, A., YADAV, A. and KUMAR, S. (2021). Joint synchronization and range estimation with correlated arrival times in molecular communication networks. *IEEE Syst. J.* 1–4. <https://doi.org/10.1109/jsyst.2023.3256061>
- MASUADI, E. (2013). Non-parametric competing risks with multivariate frailty models, PhD thesis, Oxford Brookes University, Oxford, UK <https://core.ac.uk/download/pdf/341769829.pdf>.
- MINAMI, M. (2003). A multivariate extension of inverse Gaussian distribution derived from inverse relationship. *Comm. Statist. Theory Methods* **32** 2285–2304. <https://doi.org/10.1081/sta-120025379> MR2019130
- MINAMI, M. (2007). Multivariate inverse Gaussian distribution as a limit of multivariate waiting time distributions. *J. Statist. Plann. Inference* **137** 3626–3633. <https://doi.org/10.1016/j.jspi.2007.03.038> MR2363283
- MÜLLER, H. G. (1991). Smooth optimum kernel estimators near endpoints. *Biometrika* **78** 521–530. <https://doi.org/10.1093/biomet/2f78.3.521> MR1130920
- OUIMET, F. (2022). An improvement of Tusnády’s inequality in the bulk. *Adv. in Appl. Math.* **133**. <https://doi.org/10.1016/j.aam.2021.102270> MR4340237
- OUIMET, F. (2023). A refined continuity correction for the negative binomial distribution and asymptotics of the median. *Metrika* **86** 827–849. <https://doi.org/10.1007/s00184-023-00897-2> MR4630543
- OUIMET, F. and TOLOSANA-DELGADO, R. (2022). Asymptotic properties of Dirichlet kernel density estimators. *J. Multivar. Anal.* **187** Paper No. 104832, 25 pp. <https://doi.org/10.1016/j.jmva.2021.104832> MR4319409
- PARZEN, E. (1960). *Modern Probability Theory and Its Applications*. A Wiley Publication in Mathematical Statistics. John Wiley & Sons, Inc., New York-London. MR112166
- PINHEIRO, J. C. and BATES, D. M. (1996). Unconstrained parametrizations for variance-covariance matrices. *Statistics and Computing* **6** 289–296. <https://doi.org/10.1007/bf00140873>
- RUDEMO, M. (1982). Empirical choice of histograms and kernel density estimators. *Scand. J. Statist.* **9** 65–78. MR668683

- SAHOO, S. K. and DASH, S. P. (2021). Channel parameter estimation in a molecular communication system with independent and correlated arrival times. *IEEE Wirel. Commun. Lett.* **10** 2654–2658. <https://doi.org/10.1109/lwc.2021.3110892>
- SCAILLET, O. (2004). Density estimation using inverse and reciprocal inverse Gaussian kernels. *J. Nonparametr. Stat.* **16** 217–226. <https://doi.org/10.1080/10485250310001624819> MR2053071
- SCHUSTER, E. F. (1985). Incorporating support constraints into nonparametric estimators of densities. *Comm. Statist. A—Theory Methods* **14** 1123–1136. <https://doi.org/10.1080/03610928508828965> MR797636
- SCOTT, D. W. (2015). *Multivariate Density Estimation*, Second ed. John Wiley & Sons, Inc., Hoboken, NJ. MR3329609
- SERFLING, R. J. (1980). *Approximation Theorems of Mathematical Statistics*. John Wiley & Sons, Inc., New York, NY. MR595165
- SESHADRI, V. (1999). *The Inverse Gaussian Distribution*. Springer-Verlag, New York, NY. <https://doi.org/10.1007/978-1-4612-1456-4> MR1622488
- TANG, Y., PEI, W. J., XIA, H. S. and HE, Z. Y. (2007). Multiscale entropy under the inverse Gaussian distribution: analytical results. *Chin. Phys. Lett.* **24** 1490–1493. <https://doi.org/10.1088/0256-307x/24/6/017>
- TANG, Y., PEI, W., WANG, K., HE, Z. and CHEUNG, Y. (2009). A theoretical analysis of multiscale entropy under the inverse Gaussian distribution. *Int. J. Bifurcat. Chaos* **19** 3161–3168. <https://doi.org/10.1142/s0218127409024736>
- WALD, A. (1944). On cumulative sums of random variables. *Ann. Math. Statistics* **15** 283–296. <https://doi.org/10.1214/aoms/1177731235> MR10927
- WASAN, M. T. (1968). On an inverse Gaussian process. *Skand. Aktuarietidskr.* **1968** 69–96. <https://doi.org/10.1080/03461238.1968.10413264> MR242241
- WDCG, NOSE, M., IYEMORI, T., SUGIURA, M. and KAMEI, T. (2015). Geomagnetic Dst index. <https://doi.org/10.17593/14515-74000>
- WU, X. (2019). Robust likelihood cross-validation for kernel density estimation. *J. Bus. Econom. Statist.* **37** 761–770. <https://doi.org/10.1080/07350015.2018.1424633> MR4016169
- ZHANG, X., KING, M. L. and HYNDMAN, R. J. (2006). A Bayesian approach to bandwidth selection for multivariate kernel density estimation. *Comput. Statist. Data Anal.* **50** 3009–3031. <https://doi.org/10.1016/j.csda.2005.06.019> MR2239655
- ZHANG, X., YAN, L. and LIU, Q. (2019). Adaptive target detection against spatially correlated compound-Gaussian clutter with multivariate inverse Gaussian texture. *J. Eng.* **2019** 5511–5514. <https://doi.org/10.1049/joe.2019.0142>